Copy 218
RM L52J28

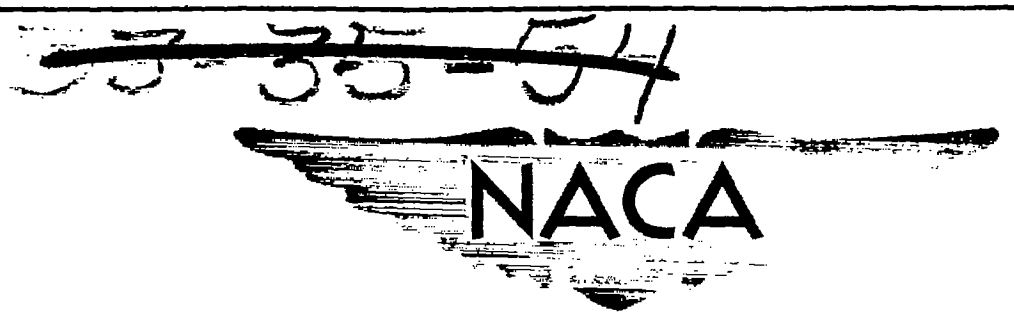

RESEARCH MEMORANDUM

CONTROL CHARACTERISTICS OF TRAILING-EDGE SPOILERS ON UNTAPERED BLUNT TRAILING-EDGE WINGS OF ASPECT RATIO 2.7 WITH 0° AND 45° SWEEPBACK AT MACH NUMBERS OF 1.41 AND 1.96

By Carl R. Jacobsen

Langley Aeronautical Laboratory
Langley Field, Va.

NATIONAL ADVISORY COMMITTEE
FOR AERONAUTICS

WASHINGTON

December 3, 1952

NATIONAL ADVISORY COMMITTEE FOR AERONAUTICS

RESEARCH MEMORANDUM

CONTROL CHARACTERISTICS OF TRAILING-EDGE SPOILERS ON UNTAPERED BLUNT TRAILING-EDGE WINGS OF ASPECT RATIO 2.7 WITH 0° AND 45° SWEEPBACK AT MACH NUMBERS OF 1.41 AND 1.96

By Carl R. Jacobsen

SUMMARY

An investigation has been made in the Langley 9- by 12-inch supersonic blowdown tunnel to determine the control characteristics of full-span trailing-edge spoilers on two related full-blunt wings (trailing-edge thickness equal to maximum wing thickness) of aspect ratio 2.7 with 0° and 45° sweepback at Mach numbers of 1.41 and 1.96. A wing similar in plan form to the unswept wing, but larger and having a partially blunt trailing edge, was also tested with a pivoted full-span trailing-edge spoiler which became detached from the surface of the wing at the higher projections. Also included are the results obtained for a spoiler located at the 70-percent-chord line of the two full-blunt wings. The results were obtained at Reynolds numbers ranging from 1.3×10^6 to 2.3×10^6.

The results of the investigation showed that the trailing-edge spoiler caused larger changes in lift, rolling moment, and pitching moment than the spoiler located at the 70-percent-chord line. The effect of the vertical gap between the pivoted spoiler and the surface of the wing at the trailing edge was to reduce sharply the rate of change of the lift increment and rolling moment with further projection. From lateral-control considerations (rolling moment, wing twisting moment, and probable hinge moment), the trailing-edge spoiler on the unswept partially blunt wing compared favorably with a 25-percent-chord trailing-edge flap.

INTRODUCTION

Previous experimental investigations at supersonic speeds have shown the rolling-moment effectiveness of spoilers to be comparable to the rolling-moment effectiveness of flap-type controls (refs. 1 and 2). Spoilers, therefore, appear promising since they might also be expected to cause less wing twisting moment (ref. 2) and have lower hinge moments

[redacted]

(ref. 3) than flap-type controls. Reference 1 has shown spoiler effectiveness to increase with rearward chordwise movement of the spoiler, indicating that the maximum effectiveness might occur at the trailing edge. For structural reasons, trailing-edge spoilers appear practical for use only on blunt trailing-edge wings. The results of references 4 and 5 indicate that a partially blunt trailing-edge wing might be used at Mach numbers of the order of 1.0 or 2.0 with little penalty in the wing aerodynamic characteristics. Calculations have further indicated that at higher Mach numbers the wing trailing edge may be thickened considerably with little or no increase in drag.

In order to obtain information concerning the control characteristics of spoilers on wings with full-blunt trailing edges at supersonic speeds, an investigation has been made of spoilers located at the trailing edge of two untapered wings of aspect ratio 2.7 with 0° and 45° sweepback. Because these full-blunt wings were expected to have excessive drag at the test Mach numbers, a trailing-edge spoiler was also tested on a wing having the same plan form as the unswept wing and a ratio of trailing-edge thickness to maximum thickness of one-third. The spoiler on this partially blunt wing was pivoted about the 85-percent-chord station and became detached from the surface of the wing at projections above 2.4 percent of the chord, thus allowing air flow between the spoiler and the wing. For comparison purposes, data were also obtained for the two full-blunt wings with spoilers located at the 70-percent-chord line.

The investigation was made at Mach numbers of 1.41 and 1.96 and at Reynolds numbers ranging from 1.3×10^6 to 2.3×10^6. Data were obtained which were applicable to positive and negative spoiler projections at angles of attack up to 25°.

COEFFICIENTS AND SYMBOLS

C_L lift coefficient, Lift/qs

C_D drag coefficient, Drag/qS

C_m pitching-moment coefficient,

$$\frac{\text{Pitching moment about } 0.25\bar{c}}{qS\bar{c}}$$

$C_{l_{gross}}$	gross rolling-moment coefficient, $\frac{\text{Rolling moment of the semispan model}}{2qSb}$
C_l	rolling-moment coefficient due to control projection, $C_{l_{gross}} - \left(C_{l_{gross}}\right)_{\frac{h}{c}=0}$
$C_{n_{gross}}$	gross yawing-moment coefficient, $\frac{\text{Yawing moment of the semispan model}}{2qSb}$
C_n	yawing-moment coefficient due to control projection, $C_{n_{gross}} - \left(C_{n_{gross}}\right)_{\frac{h}{c}=0}$
$\Delta C_L, \Delta C_D, \Delta C_m$	increments in lift, drag, and pitching-moment coefficients due to spoiler projection
P_b	base pressure coefficient
q	free-stream dynamic pressure, lb/sq in.
S	semispan wing area, sq in.
c	wing chord, in.
$\bar{c}$	mean aerodynamic chord, in.
b	wing span, twice distant from wing root chord to wing tip, in.
h	spoiler projection measured from wing surface in a plane normal to chord line, positive when located on upper surface, in.
α	angle of attack, deg
R	Reynolds number based on $\bar{c}$

[redacted]

MODELS

The three semispan-wing models of solid steel which were tested (designated A, B, and C and seen in figs. 1 and 2) had untapered plan forms with aspect ratios of 2.7 and symmetrical, 6-percent-thick, flat-sided sections with leading-edge wedges which extended to the 40-percent-chord station. Wing A was unswept and had a full-blunt trailing edge (fig. 1). Wing B was swept back 45° but, otherwise, was identical to wing A. The spoilers located at the trailing edge and at the 70-percent-chord line of wings A and B extended from the wing-fuselage intersection at $0.165b/2$ to the wing tip. Control projections were simulated by progressively machining the 0.028-inch-thick brass spoilers from an initial projection of 6 percent of the chord down to each desired height. Pressure orifices to measure the base pressure of wing A were located at 23, 47, 71, and 95 percent of the exposed semispan.

Wing C (figs. 2 and 3) was similar to wing A but was larger and had the trailing edge beveled to a 2-percent-chord thickness. The trailing-edge spoiler for wing C pivoted about the 85-percent-chord station and extended from the wing-fuselage juncture at $0.11b/2$ to the wing tip.

TUNNEL

The Langley 9- by 12-inch supersonic blowdown tunnel in which the present tests were made utilizes the compressed air of the Langley 19-foot pressure tunnel. The air enters at an absolute pressure of about $2\frac{1}{3}$ atmospheres. To insure condensation-free flow, the air is passed through a silica-gel dryer, and then through banks of finned electrical heaters. The criteria for the amount of drying and heating necessary for condensation-free flow were obtained from reference 6. The two test section Mach numbers are provided by interchangeable nozzle blocks. The free-stream Mach numbers have been calibrated at 1.41 ± 0.02 and 1.96 ± 0.02. The corresponding static-pressure variations were about ± 2.0 percent at $M = 1.41$ and ± 2.2 percent at $M = 1.96$. The deviation in stream angle for the tunnel clear condition was $\pm 0.25°$ at $M = 1.41$ and $\pm 0.20°$ at $M = 1.96$. The results of the tunnel calibration tests (ref. 7) were used in determining the dynamic pressures which were used in reducing the data.

The average dynamic pressure and Reynolds number at each Mach number for the three models are as follows:

Mach number	q (lb/sq in.)	Reynolds number for -	
		Wings A and B	Wing C
1.41	12.0	1.6×10^6	2.3×10^6
1.96	10.5	1.3	1.9

The test Reynolds number decreased about 2 percent during the course of each run because of the decreasing pressure of the inlet air.

TEST TECHNIQUE

The semispan models used in this investigation were cantilevered from a strain-gage balance which mounts flush with the tunnel wall and rotates with the model through the angle-of-attack range. A test body was attached to each of the wings and loads were measured on the wing-body combinations. The test body consisted of a half-body of revolution and a 0.25-inch shim which was used to raise the half-body of revolution off the tunnel wall and thus minimize the effects of the tunnel-wall boundary layer on the flow over its surface (ref. 8). Because of the balance deflection under load, a gap of about 0.010 inch was maintained between the test body and the tunnel wall under a no-load condition. The rolling- and yawing-moment axes were located at the electrical center of the balance (see figs. 1 and 2).

All three wing models were originally tested both with and without transition strips. Because of test difficulties, the only final data obtained were those without transition strips for the full-blunt wings, A and B, and those with transition strips for wing C. The transition-fixed data for wing C were obtained with a 0.033c band of carborundum grains having maximum dimensions of about 0.004 inch with the forward edge of the band located 0.065c behind the wing leading edge. The investigation was made at angles of attack which varied from -26° to 25° and at spoiler projections which varied from 0 to 10 percent of the wing chord. Complete data for all wing and spoiler configurations, however, were obtained only at angles of attack from -6° to 8° and at spoiler projections from 0 to 6 percent of the wing chord. The angle-of-attack range at $M = 1.41$ was necessarily more limited than at $M = 1.96$ because of tunnel blockage and shock-interference effects.

ACCURACY

No tare corrections have been applied to any of the data presented. From a general consideration of balance-calibration accuracy and repeatability of data, the accuracy of the measurement of forces and moments, in terms of coefficients, are believed to be about as follows:

C_L	±0.005
C_l	±0.001
C_D	±0.001
C_m	±0.002
C_n	±0.0002

The angle-of-attack values are believed to be accurate within ±0.05°, based upon the limitations of the mechanical angle-of-attack system and the calibration charts from which the actual values were obtained.

RESULTS AND DISCUSSION

Variations of the lift, rolling-moment, and pitching-moment coefficients of the semispan models with projection of spoilers located at the trailing edge of the three wings are presented in figures 4 to 6 for various angles of attack. These force and moment measurements are presented primarily to show samples of the basic data as the measurements include loads on a somewhat arbitrary test body and are, therefore, not directly applicable to configurations including more conventional body arrangements. It is believed, however, that the use of a different body arrangement would not qualitatively affect the data. The range of test variables for the two wings, A and B, with the 70-percent-chord-station spoilers (not presented) was essentially the same as that for the trailing-edge spoilers. Base pressure measurements obtained along the trailing edge of wing A (unswept full-blunt wing) both with and without a 6-percent-chord-height spoiler are presented in figure 7.

Because the models are symmetrical the data obtained in the negative angle-of-attack range were also applicable to negative spoiler projections at positive angles of attack. The data contained in figures 4 to 7 are, therefore, presented at representative positive angles of attack in figures 8 and 9. Comparable force data for the spoiler located at the 70-percent-chord line of the two full-blunt wings, A and B, along with complete incremental-drag and yawing-moment data are also included in these figures. For the few very limited cases in which data were obtained for the wings both with and without transition strips, the data indicated that the attempt to fix the transition had little effect on the incremental loads caused by the projected spoiler. The trailing-edge spoiler-base-drag and wing-base-drag increments due to spoiler

projection obtained on the unswept full-blunt wing by integration of the base pressures contained in figure 7 are included with the drag data in figure 8.

Unswept Wings

Lift and rolling moment.- All spoilers on the two unswept wings produced substantial lift increments (fig. 8(a)) and rolling moments (fig. 8(b)) throughout the angle-of-attack range. Usually the lift increments and rolling moments decreased for upper-surface projections and increased for lower-surface projections as the angle of attack was increased, thus indicating little change in the lift increment and the rolling moment for differentially projected spoilers with increasing angle of attack. The lift increments and rolling-moment effectiveness of the pivoted spoiler on the partially blunt wing at $M = 1.41$ were slightly less than those of the trailing-edge spoiler on the full-blunt wing for projections below that at which a vertical gap occurred between the pivoted spoiler and the surface of the wing $\left(\frac{h}{c} = \pm 0.024\right)$. At angles of attack of 4°, 8°, and 14°, and at $M = 1.96$, the lift increments and rolling-moment effectiveness of the pivoted spoiler on the partially blunt wing were essentially the same as those of the trailing-edge spoiler on the full-blunt wing at projections below that for which the vertical gap occurred. Beyond this projection these values were substantially less than what they were for the trailing-edge spoiler on the full-blunt wing. The spoiler on the partially blunt wing was projected up to 10 percent, but there was practically no difference between the lift increments and rolling moments at 6 and 10 percent projection (see fig. 6). Consequently, the data from 6 to 10 percent projection were omitted from these figures.

For equal spoiler projections on the full-blunt wings, the trailing-edge spoiler in most cases had about twice the effect on lift increment and rolling moment as the spoiler at the 70-percent-chordwise station. The pivoted spoiler also had more effect prior to the occurrence of the vertical gap and in several cases it had more effect up to 6 percent projection than the spoiler at the 70-percent-chordwise station.

A general illustration of the effect of a spoiler on the flow over a wing, based upon the pressure-distribution measurements of reference 1, is presented in figure 10. The dashed areas ahead of and behind the spoiler indicate approximate dead-air regions. These dead-air regions are usually accompanied by a flow compression ahead of and a flow expansion behind the spoiler. Generally, the magnitude of the negative loading resulting from the compression exceeded the magnitude of the positive loading resulting from the expansion. From figure 10, it can be seen that the differences previously noted between the effects of the

[redacted]

trailing-edge spoiler and the spoiler at the 70-percent-chordwise station on the full-blunt wing were directly related to the absence of any loading behind the trailing-edge spoiler to offset the large loading ahead of it.

Pitching moment.- The pitching-moment increments were very large for the trailing-edge spoilers as compared with the corresponding values for the spoiler at the 70-percent-chord station. These large increments in pitching moment for the trailing-edge spoiler might be undesirable because of the associated high-wing twisting moments. It may be seen from figure 10 that the differences in pitching-moment increment due to spoiler chordwise location were directly related to the decrease in loading behind the spoiler as it was moved back to the trailing edge. The pitching-moment increments of the pivoted spoiler on the partially blunt wing, wing C, were less than at $M = 1.41$ and about the same at $M = 1.96$ as for the trailing-edge spoiler on the full-blunt wing, wing A, at projections below that for which the vertical gap occurred between the pivoted spoiler and the surface of the wing $\left(\frac{h}{c} = \pm 0.024\right)$. Beyond this point the pitching-moment increments changed only slightly in much the same manner as did the lift increments and rolling moments.

For the trailing-edge spoilers, the pitching-moment increments usually decreased for upper-surface spoiler projections and increased for lower-surface projections as the angle of attack was increased. The variation of these increments at high projections for the full-blunt wing was large enough that, for differentially projected spoilers on opposite wings, an appreciable longitudinal change in trim at moderate to high angles of attack might result. Somewhat smaller trim changes are also indicated for the 70-percent-chord-station spoiler. These trim changes are more pronounced at a Mach number of 1.41 and at high angles of attack because of reversals in pitching moment of the lower-surface spoiler.

Drag and yawing moment.- Generally, the drag increments and yawing moments for the pivoted spoiler (figs. 8(d) and 8(e)) were considerably less than they were for the spoilers on the full-blunt wing. These values compare more realistically, however, when it is realized that the frontal area of the partially blunt wing (wing C) was not increased until after the spoiler was projected above the boattailed section $\left(\frac{h}{c} = \pm 0.02\right)$.

The incremental drag and yawing moments decreased for an upper-surface projection and increased for a lower-surface projection as the angle of attack was increased. The base drag of the spoiler on the full-blunt wing at zero angle of attack ranged from 10 and 11 percent of the total drag increment at Mach numbers of 1.41 and 1.96, respectively, to about twice that at 8° angle of attack. These percentages illustrate,

as would be expected from shock-expansion theory, that more drag was caused by the compression of the flow ahead of the spoiler than by the expansion of the flow behind it. The increment in wing base drag due to spoiler projection was insignificant throughout the angle-of-attack range at both Mach numbers.

45° Sweptback Wing

For the trailing-edge spoiler, the values of lift increment, rolling-moment, and pitching-moment increment (figs. 9(a), 9(b), and 9(c), respectively), in general, decreased for an upper-surface projection and remained fairly constant or increased slightly for a lower-surface projection with increasing angle of attack. For this trailing-edge spoiler, the lift, rolling-moment, and pitching-moment trends for upper- and lower-surface spoilers were about the same for the swept wing as they were for the unswept wing. The spoiler, however, usually had slightly less effect on lift, rolling moment, and pitching moment for the swept wing than for the unswept wing. For the 70-percent-chord-station spoiler projected from the upper surface, the values of lift increment and rolling moment were generally half or less than what they were for the trailing-edge spoiler. For lower-surface projections, however, reversals in lift increment and rolling moment were obtained with small spoiler projections at moderate angles of attack and with all spoiler projections at high angles of attack. Reversals in pitching-moment increment caused by the projected 70-percent-chord-station spoiler were obtained with both upper- and lower-surface projections at small angles of attack. These pitching-moment reversals for upper-surface spoiler projections gradually disappeared with increasing angle of attack until there were no reversals at angles of attack above 8°. For the swept wing, the 70-percent-chord-station spoilers on the lower surface or differentially projected 70-percent-chord-station spoilers on opposite wings do not provide nearly as satisfactory lift, rolling-moment, and pitching-moment changes as they do for the unswept wing.

For the trailing-edge spoiler, the drag increments and yawing moments (figs. 9(d) and 9(e), respectively) decreased for an upper-surface projection and increased for a lower-surface projection as the angle of attack was increased. Generally, these trends were similar to those for the unswept wing, but the amount of variation with spoiler projection was less in magnitude for drag and slightly greater in magnitude for yawing moment. For the 70-percent-chord-station spoiler, however, the variations of drag increment and yawing moment with angle of attack were, in general, somewhat different from those for the unswept wing.

Comparison of Spoiler Data With Flap Data

The following table illustrates the effect of spoilers and flaps on the aerodynamic characteristics of two wings at an angle of attack of 0°:

Wing	Control	h/c	δ, deg	ΔC_L	C_l	ΔC_m	ΔC_D
Partially blunt	Flap	-0.04	5.7	0.041	0.0054	-0.0220	0.0025
Partially blunt	Spoiler			.041	.0054	-.0240	.0134
Reference 9	Flap	-.04	6.3	.031	.0043	-.0174	.0041
Reference 1	Spoiler			.031	.0043	-.0067	.0244

Included in the table are values obtained for a full-span, 25-percent-chord, trailing-edge flap on the partially blunt wing of the present investigation at M = 1.96 (unpublished) and on an unswept wing having an aspect ratio of 2.5, a taper ratio of 0.625, and 6-percent hexagonal airfoil sections at M = 1.90 (ref. 9). Also included are values for the trailing-edge spoiler on the partially blunt wing of the present investigation at M = 1.96 and values obtained at M = 1.90 from reference 1 by using the 55-, 65-, and 75-percent-chord-station spoiler data to interpolate for a 70-percent-chord-station spoiler. (The same wing was used in both refs. 1 and 9.) The force and moment coefficients obtained from references 1 and 9 which were based on exposed wing area and a pitching-moment axis located at $0.5\bar{c}$ have been altered to conform to the definitions given in the present paper. These coefficients, however, should not be directly compared with the coefficients obtained in the present investigation for the 70-percent-chord-station spoilers, primarily because the measurements were obtained from a wing mounted in the presence of a body and not from a wing-body combination as was done herein. Also, a small gap existed between the wing and body for the investigations of references 1 and 9 in addition to the wing airfoil section being different from the airfoil section of the unswept full-blunt wing of the present investigation. It can be seen from the table that, for equal lift increments and rolling moment $(\Delta C_L, C_l)$, the spoilers caused considerably more drag than did the flaps. It is interesting to note that for the partial-blunt wing the pitching-moment increments (and, consequently, the wing twisting moments) for the trailing-edge spoiler are only slightly higher than for the flap. This would indicate one possible advantage of using spoilers, in that the hinge moments would be expected to be lower for the spoiler than for the flap. It should be pointed out that, for equal rolling-moment effectiveness $(C_l = 0.0054)$, the pitching-moment increments for the trailing-edge spoiler on the unswept full-blunt wing are higher than for the partially blunt wing (-0.0330 as compared with -0.0240). The

data, however, indicate these values to be more nearly equal at angles of attack greater than 0°. Consequently, this spoiler should also compare favorably with a flap since the variation of pitching-moment increment with flap deflection was about independent of angle of attack. The table shows the pitching moment for the 70-percent-chord-station spoiler to be lower than for the flap which would indicate a distinct advantage over the flap; however, as was pointed out, this spoiler was not as effective as the trailing-edge spoiler.

It will be noted in the table that about 6° flap deflection are required to produce the same effectiveness as a spoiler projected 4 percent of the wing chord. This result would indicate one possible disadvantage in using spoiler, in that flap deflections in excess of 6° are known to be practical, whereas spoiler projections in excess of the thickness of the wing may involve structural problems.

CONCLUDING REMARKS

An investigation has been made in the Langley 9- by 12-inch supersonic blowdown tunnel to determine the control characteristics of full-span trailing-edge spoilers on several blunt trailing-edge wings of aspect ratio 2.7 at Mach numbers of 1.41 and 1.96. The results showed that the spoiler was more effective when located at the trailing edge of an unswept or 45° sweptback wing than when located at the 70-percent-chord line. The spoiler, when located at the 70-percent-chord line of the unswept wing, was effective in producing rolling moment; but when located at the 70-percent-chord line of the swept wing, the spoiler was not nearly as effective and tended to reverse for lower-surface projections with increasing angle of attack.

The effect of the vertical gap between the pivoted spoiler and the surface of the wing at the trailing edge was to reduce sharply the rate of change of the lift increment and rolling moment with projection above a gap of about 2 percent chord.

From lateral-control considerations (rolling moment, wing twisting moment, and probable hinge moments), the trailing-edge spoiler on the unswept partially blunt wing compared favorably with a 25-percent-chord trailing-edge flap.

Langley Aeronautical Laboratory,
National Advisory Committee for Aeronautics,
Langley Field, Va.

REFERENCES

1. Conner, D. William, and Mitchell, Meade H., Jr.: Effects of Spoiler on Airfoil Pressure Distribution and Effects of Size and Location of Spoilers on the Aerodynamic Characteristics of a Tapered Unswept Wing of Aspect Ratio 2.5 at a Mach Number of 1.90. NACA RM L50L20, 1951.

2. Hammond, Alexander D.: Lateral-Control Investigation of Flap-Type and Spoiler-Type Controls on a Wing With Quarter-Chord-Line Sweepback of 60°, Aspect Ratio 2, Taper Ratio 0.6, and NACA 65A006 Airfoil Section. Transonic-Bump Method. NACA RM L50E09, 1950.

3. Fikes, Joseph E.: Hinge Moment and Other Aerodynamic Characteristics at Transonic Speeds of a Quarter-Span Spoiler on a Tapered 45° Sweptback Wing of Aspect Ratio 3. NACA RM L52A03, 1952.

4. Chapman, Dean R.: Reduction of Profile Drag at Supersonic Velocities by the Use of Airfoil Sections Having a Blunt Trailing Edge. NACA RM A9H11, 1949.

5. Cleary, Joseph W., and Stevens, George L.: The Effects at Transonic Speeds of Thickening the Trailing Edge of a Wing With a 4-Percent-Thick Circular-Arc Airfoil. NACA RM A51J11, 1951.

6. Burgess, Warren C., Jr., and Seashore, Ferris L.: Criterions for Condensation-Free Flow in Supersonic Tunnels. NACA TN 2518, 1951.

7. May, Ellery B., Jr.: Investigation of the Effects of Leading-Edge Chord-Extensions on the Aerodynamic and Control Characteristics of Two Sweptback Wings at Mach Numbers of 1.41, 1.62, and 1.96. NACA RM L50L06a, 1951.

8. Conner, D. William: Aerodynamic Characteristics of Two All-Movable Wings Tested in the Presence of a Fuselage at a Mach Number of 1.9. NACA RM L8H04, 1948.

9. Mitchell, Meade H., Jr.: Effects of Varying the Size and Location of Trailing-Edge Flap-Type Controls on the Aerodynamic Characteristics of an Unswept Wing at a Mach Number of 1.9. NACA RM L50F08, 1950.

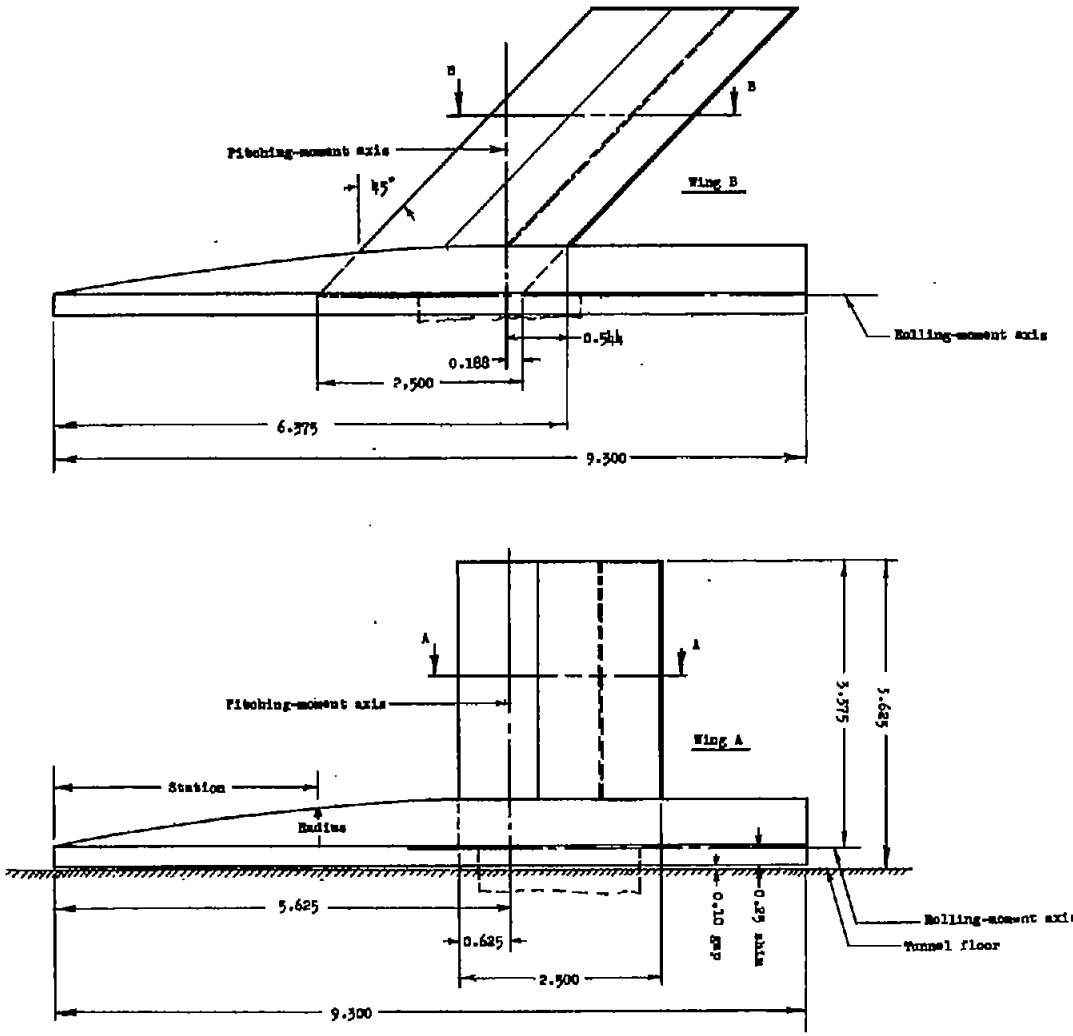

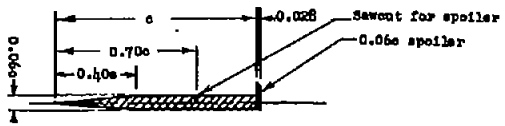

Body	Ordinates
Station	Radius
0.000	0.000
0.541	.095
1.082	.180
1.623	.260
2.165	.330
2.706	.391
3.247	.441
3.788	.490
4.330	.519
4.870	.538
5.412	.541
9.300	.544

NACA

Figure 1.- Details of semispan-wing models with trailing-edge spoilers.
All dimensions are in inches.

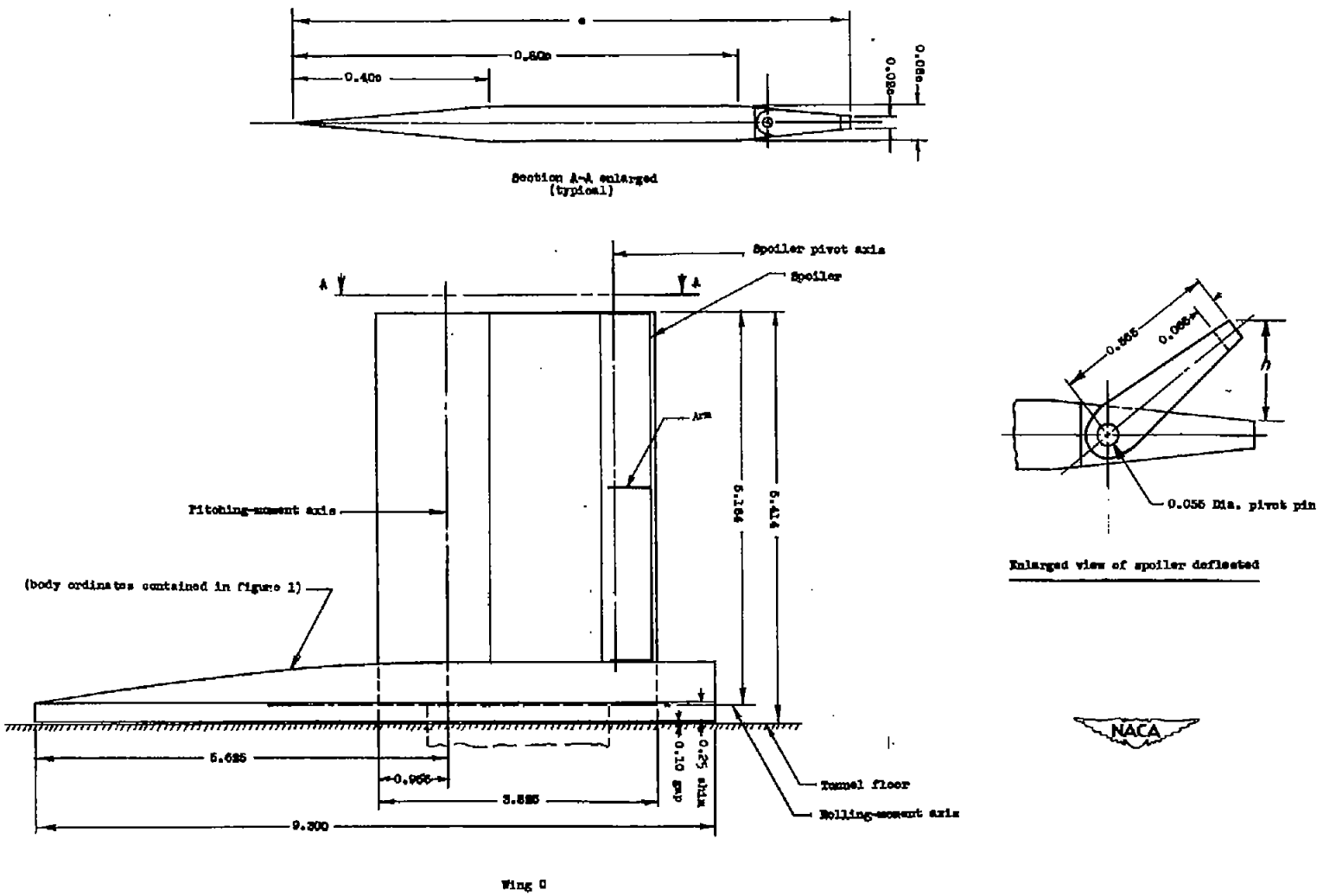

Figure 2.- Details of semispan-wing model with pivoted trailing-edge spoiler. All dimensions are in inches.

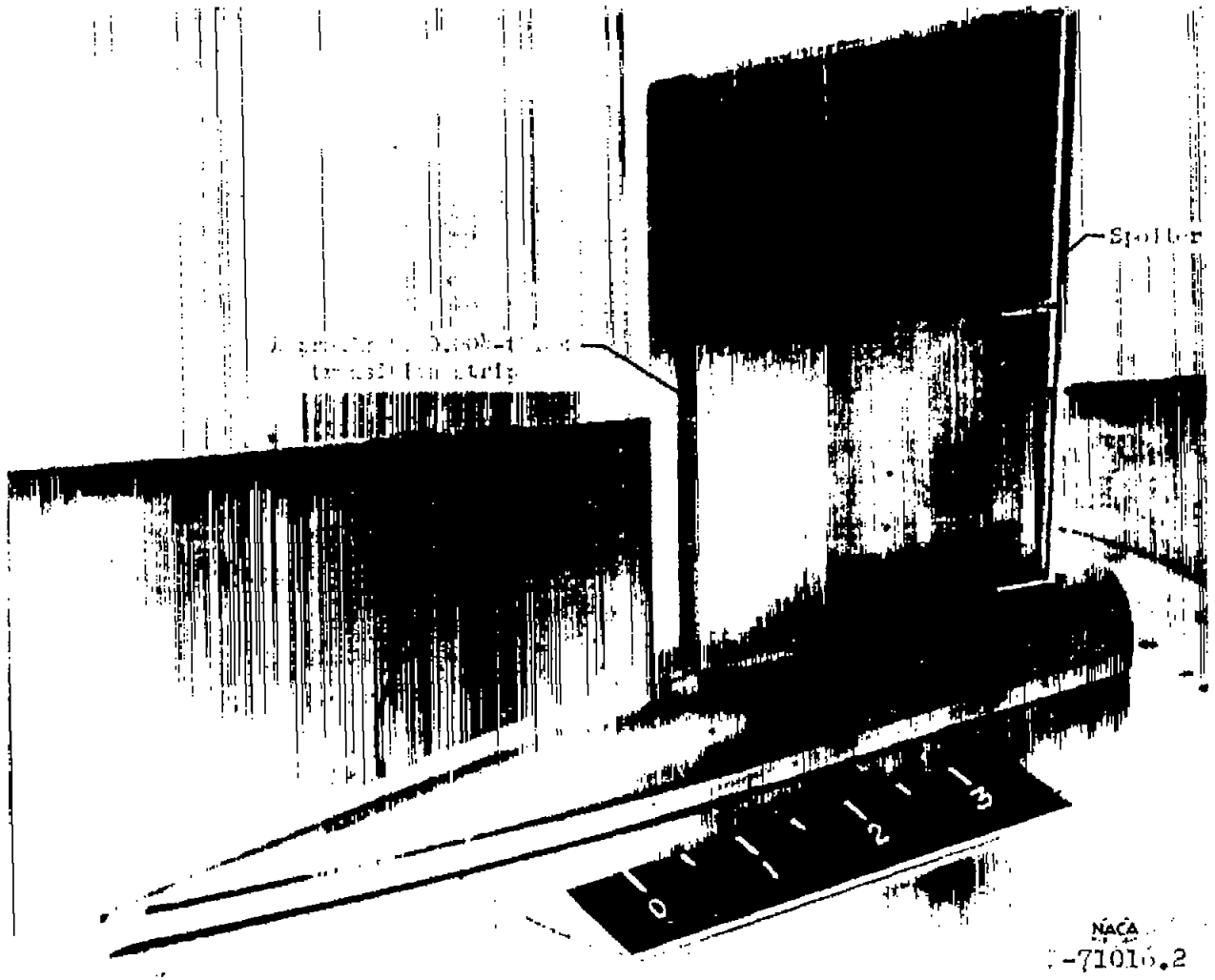

Figure 3.- Photograph of semispan-wing model with pivoted trailing-edge spoiler deflected. All dimensions are in inches.

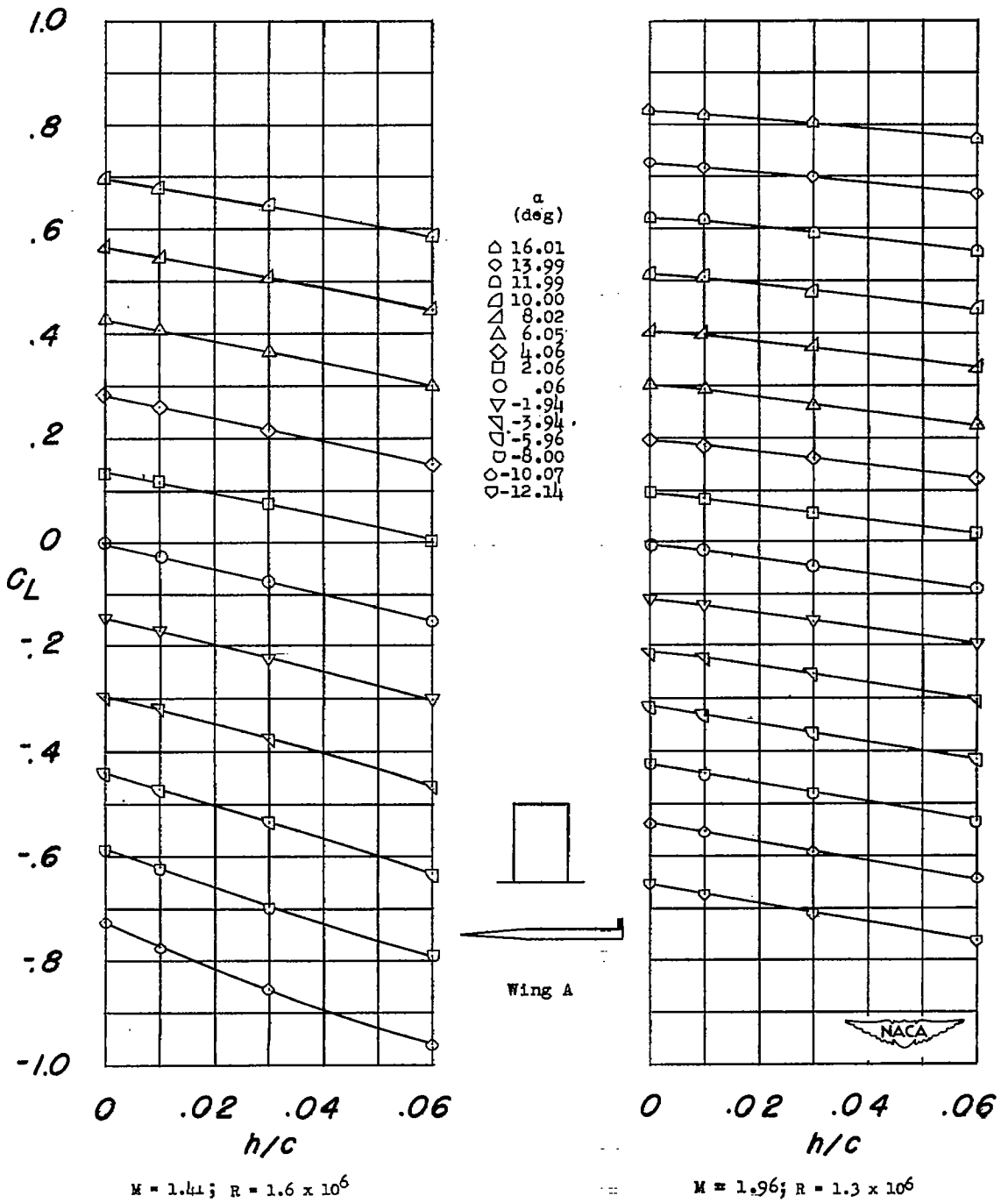

(a) Lift.

Figure 4.- Aerodynamic characteristics of an unswept semispan wing with a trailing-edge spoiler.

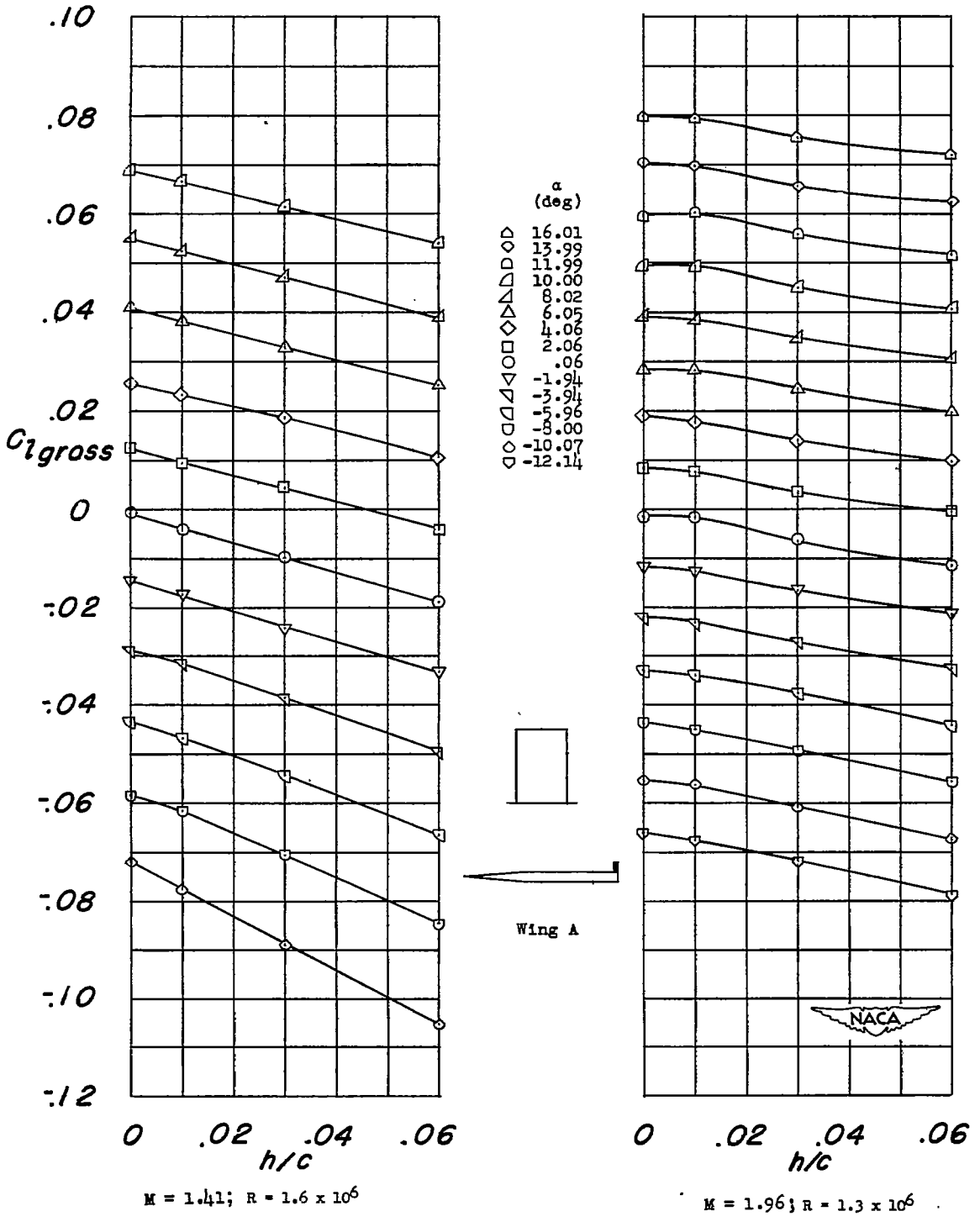

(b) Gross rolling moment.

Figure 4.- Continued.

[redacted]

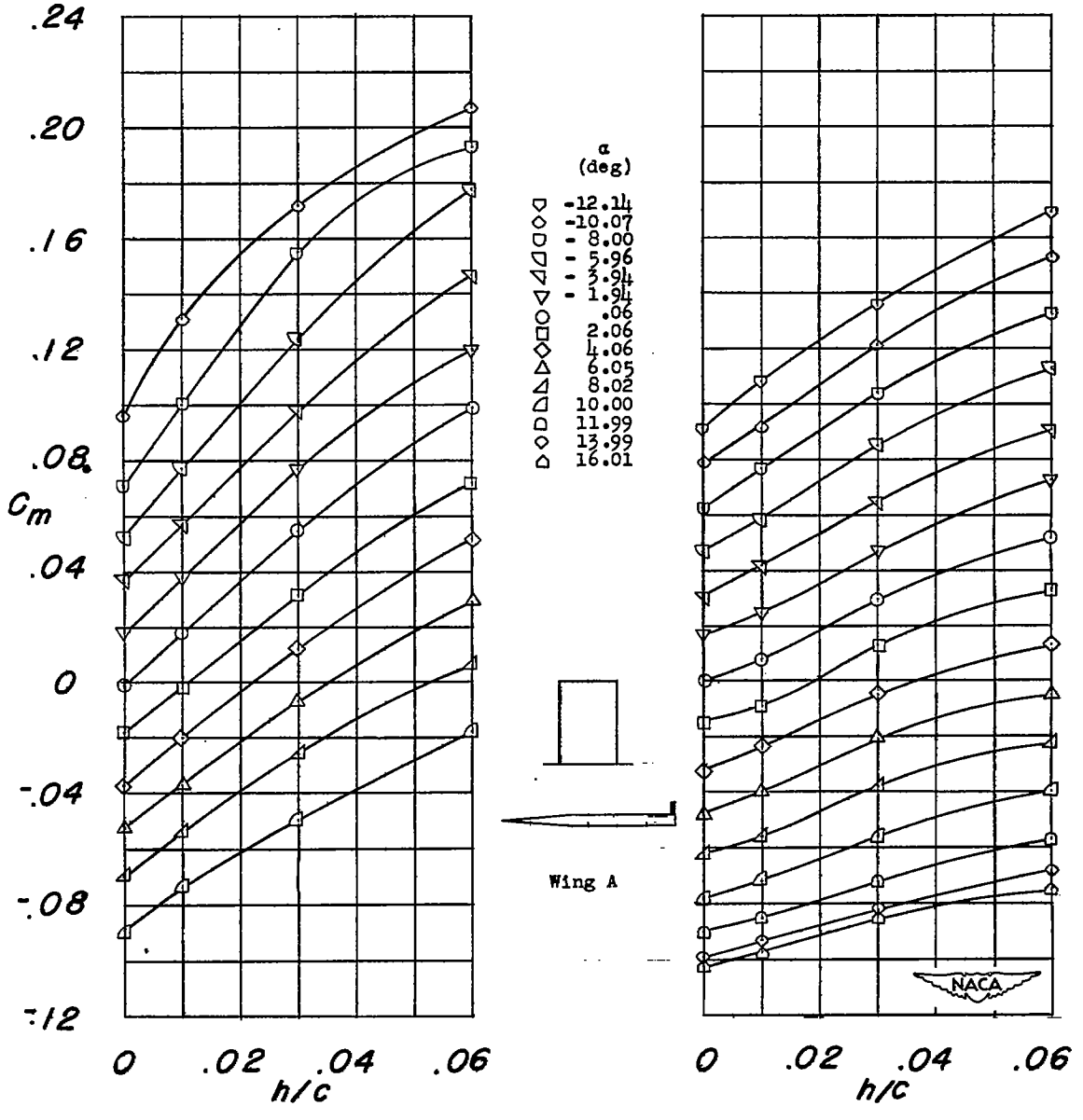

M = 1.41; R = 1.6 x 10^6 M = 1.96; R = 1.3 x 10^6

(c) Pitching moment.

Figure 4.- Concluded.

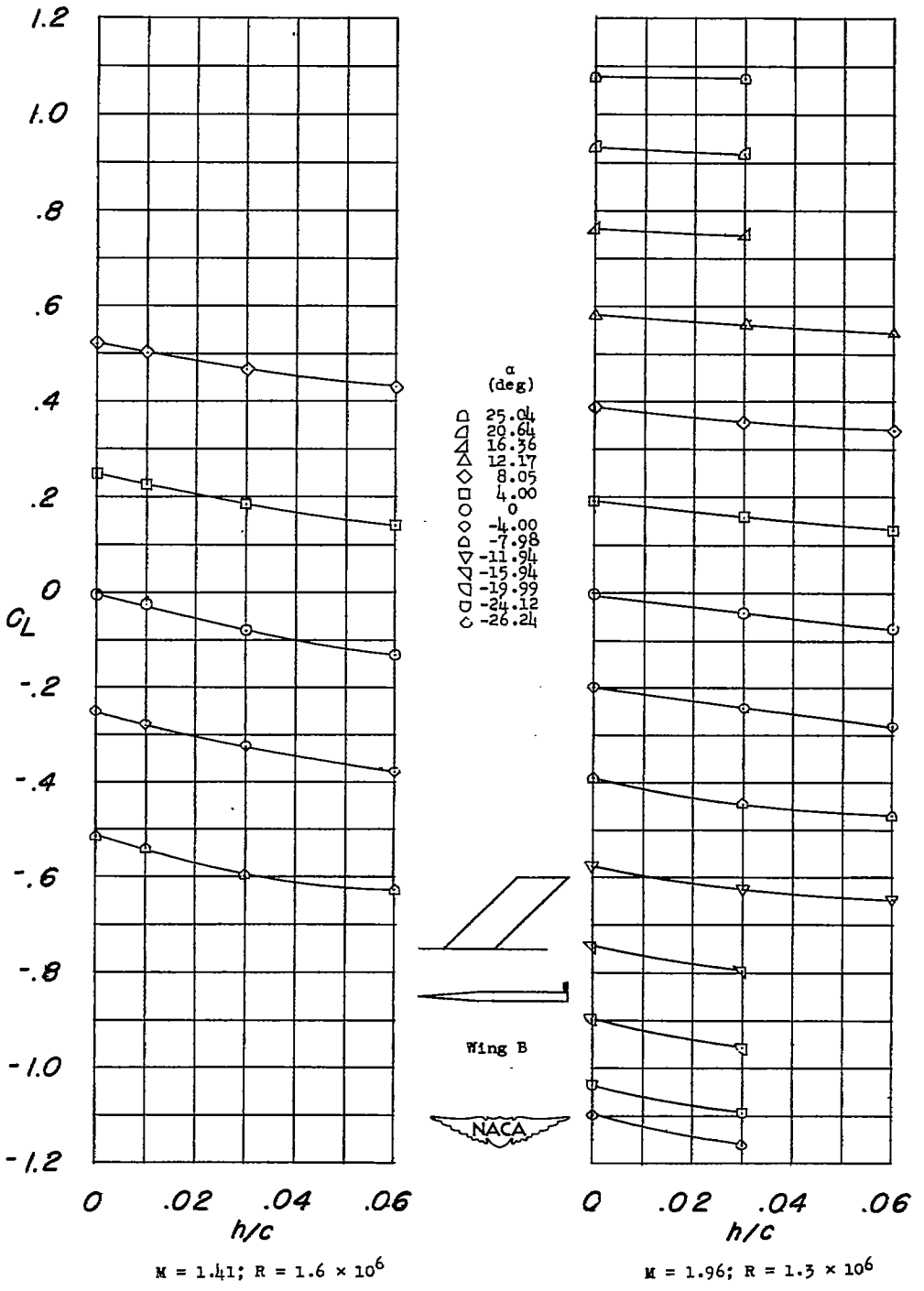

(a) Lift.

Figure 5.- Aerodynamic characteristics of a 45° sweptback semispan wing with a trailing-edge spoiler.

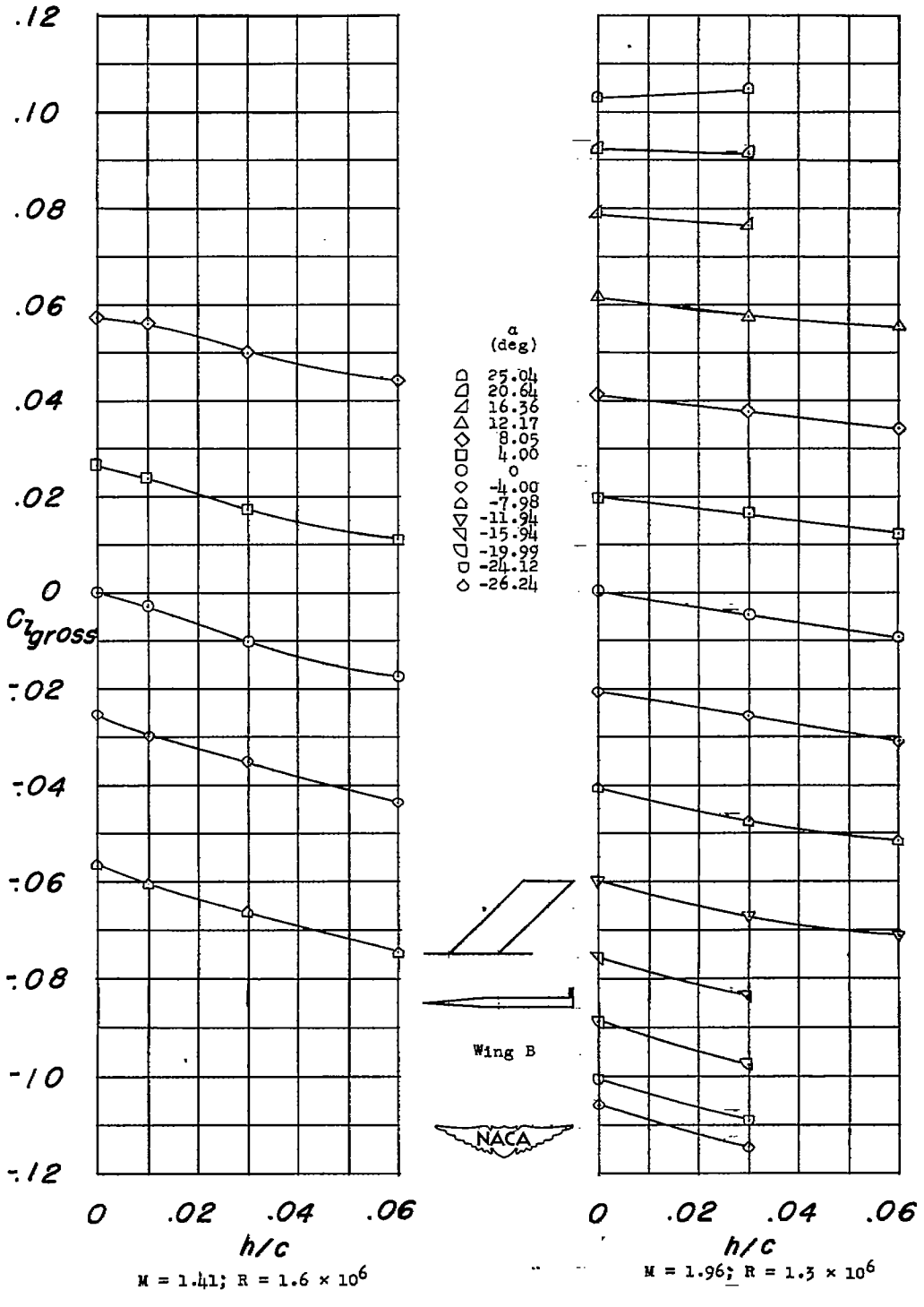

(b) Gross rolling moment.

Figure 5.- Continued.

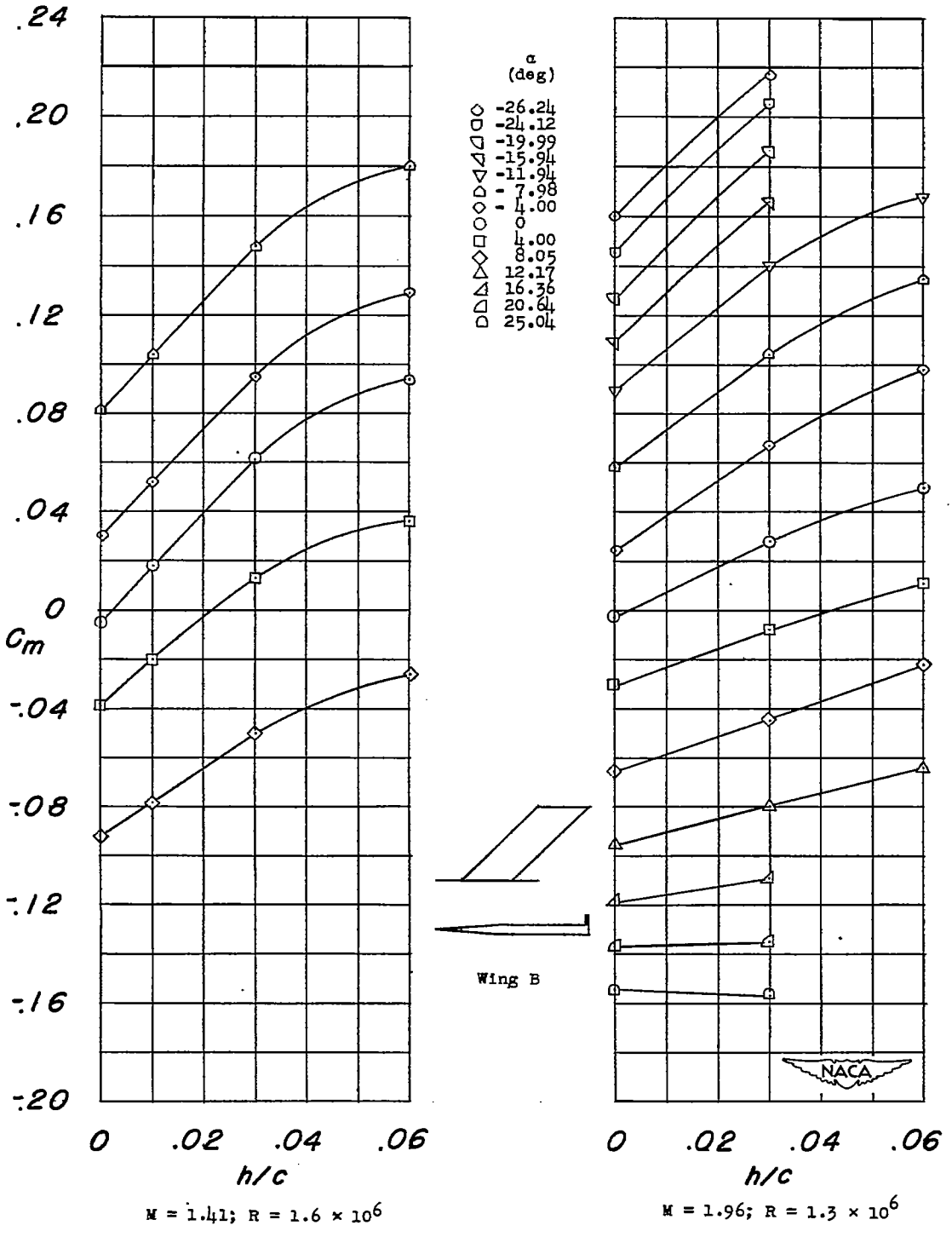

(c) Pitching moment.

Figure 5.- Concluded.

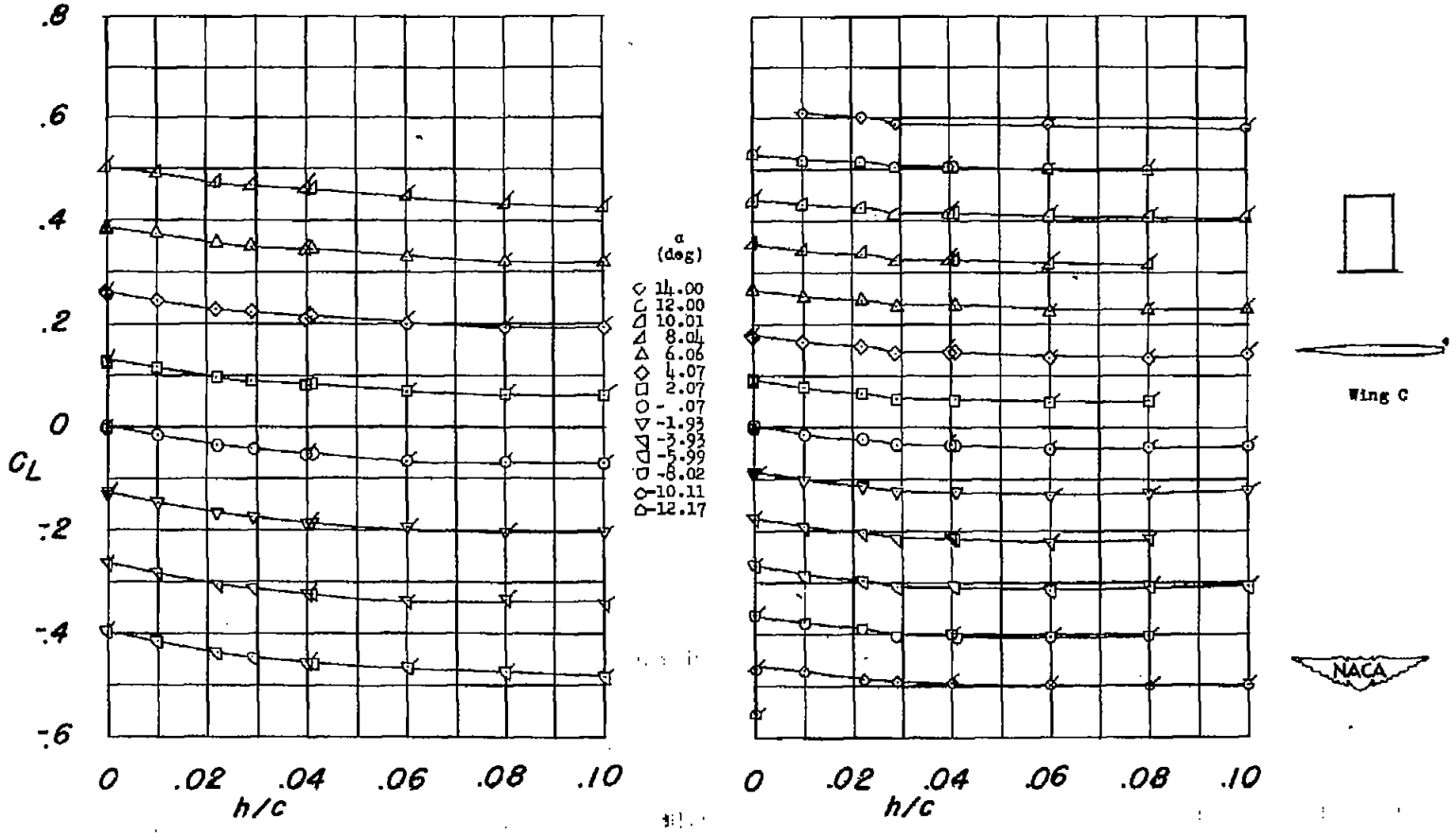

(a) Lift.

Figure 6.- Aerodynamic characteristics of an unswept wing (with transition strips) with a pivoted trailing-edge spoiler. Flagged symbols denote data obtained at a different date from original data.

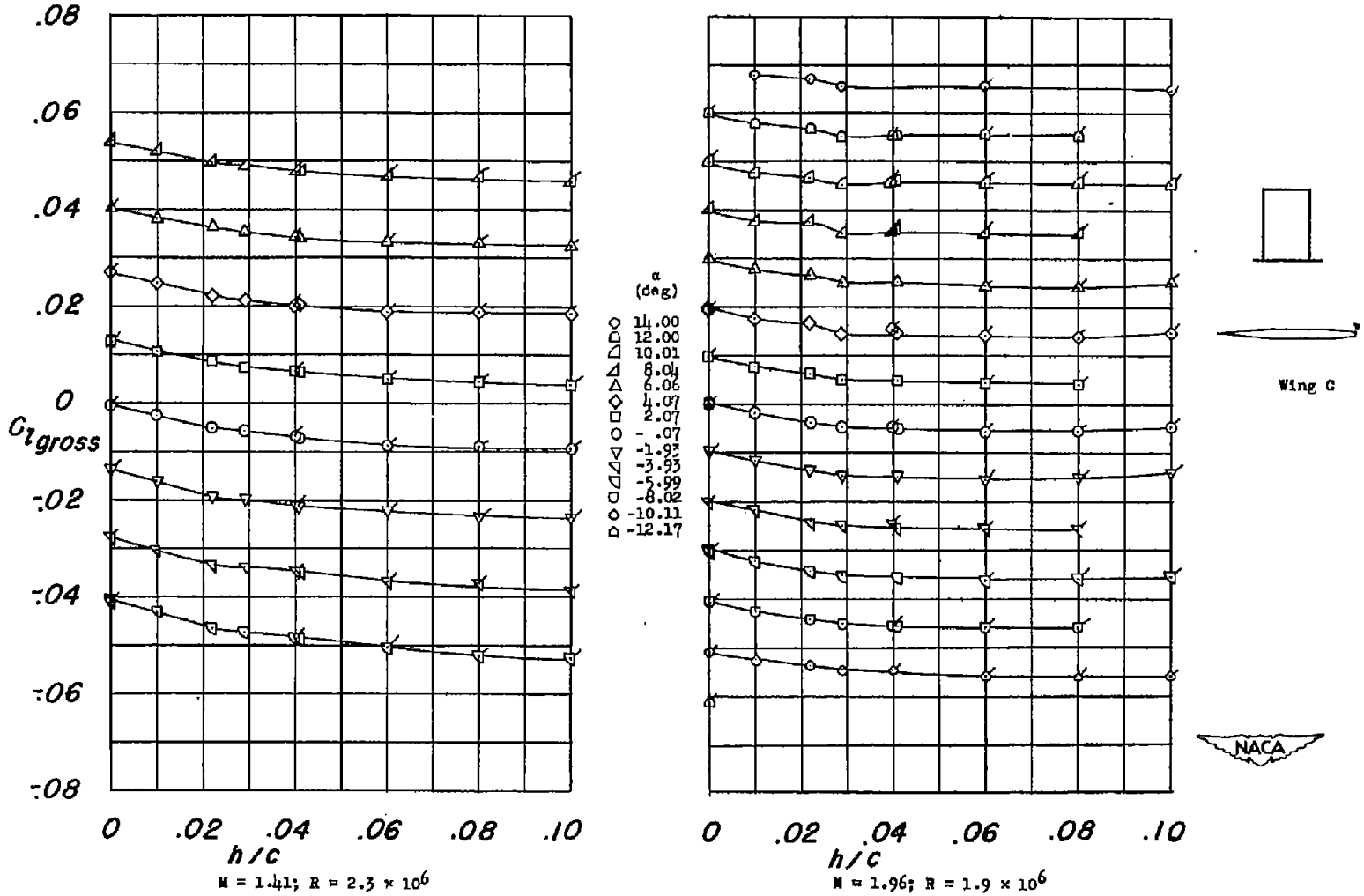

(b) Gross rolling moment.

Figure 6.- Continued.

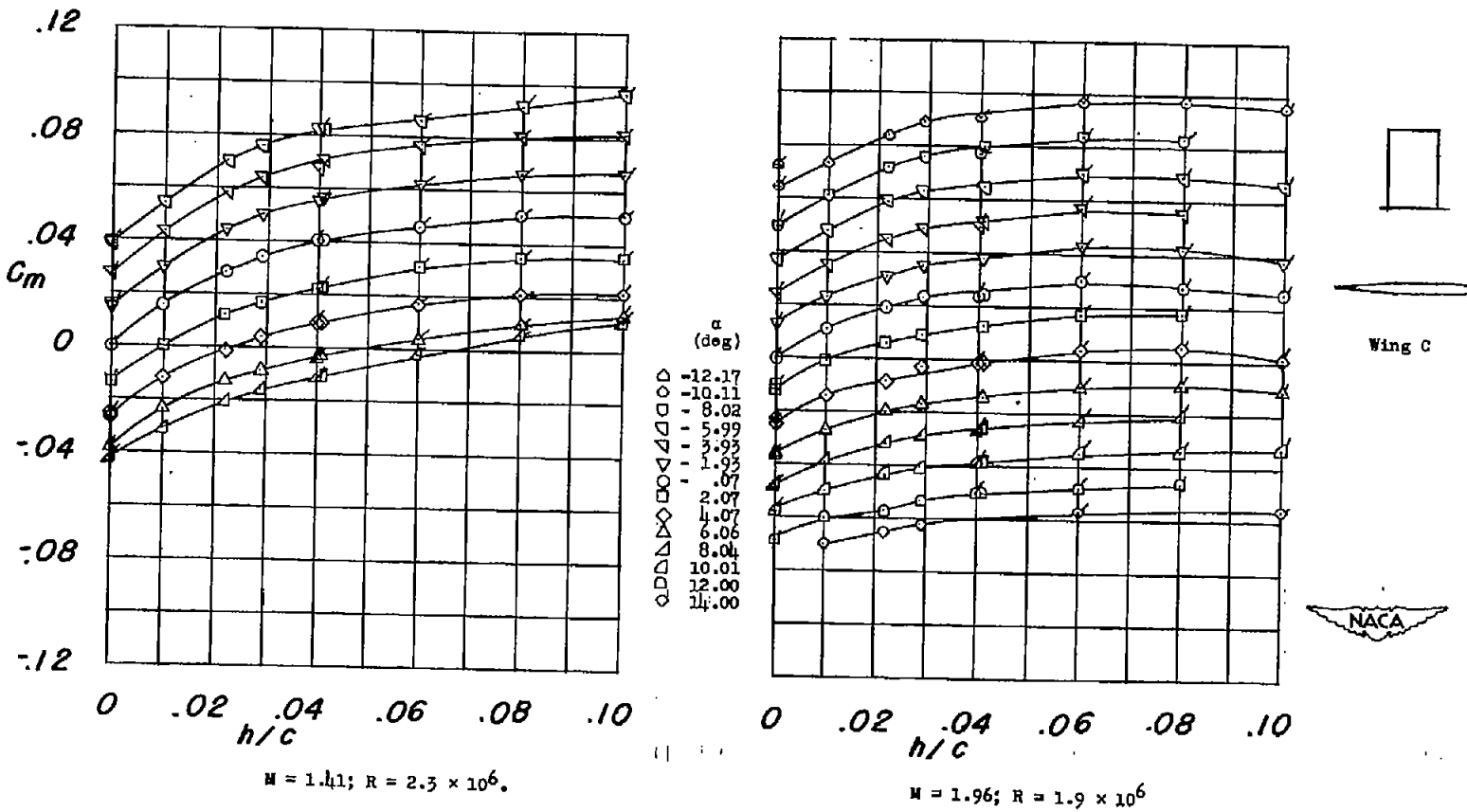

(c) Pitching moment.

Figure 6.- Concluded.

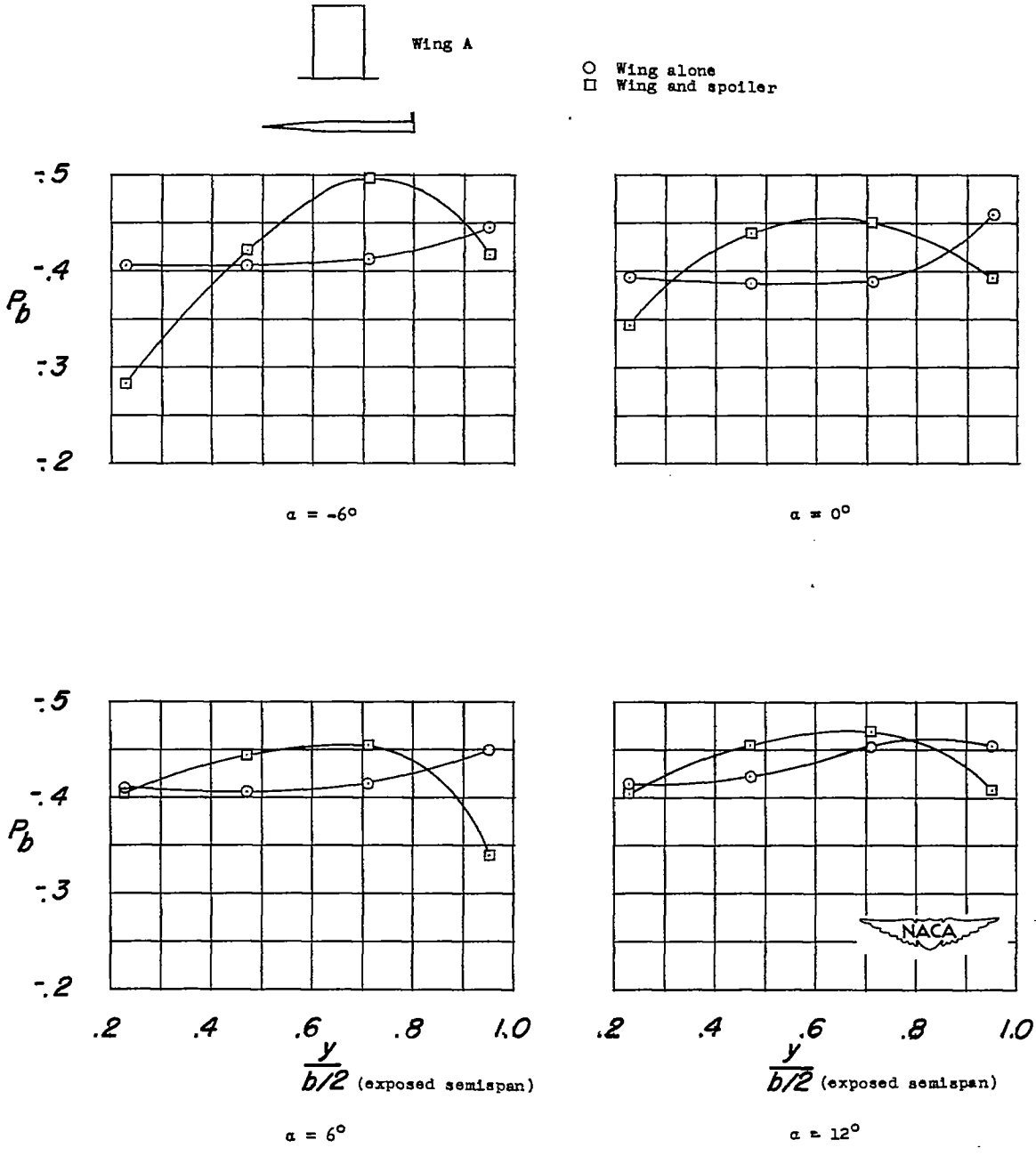

(a) M = 1.41; R = 1.6×10^6.

Figure 7.- Effects of a trailing-edge spoiler projected 0.06c on the base pressure of an unswept semispan wing.

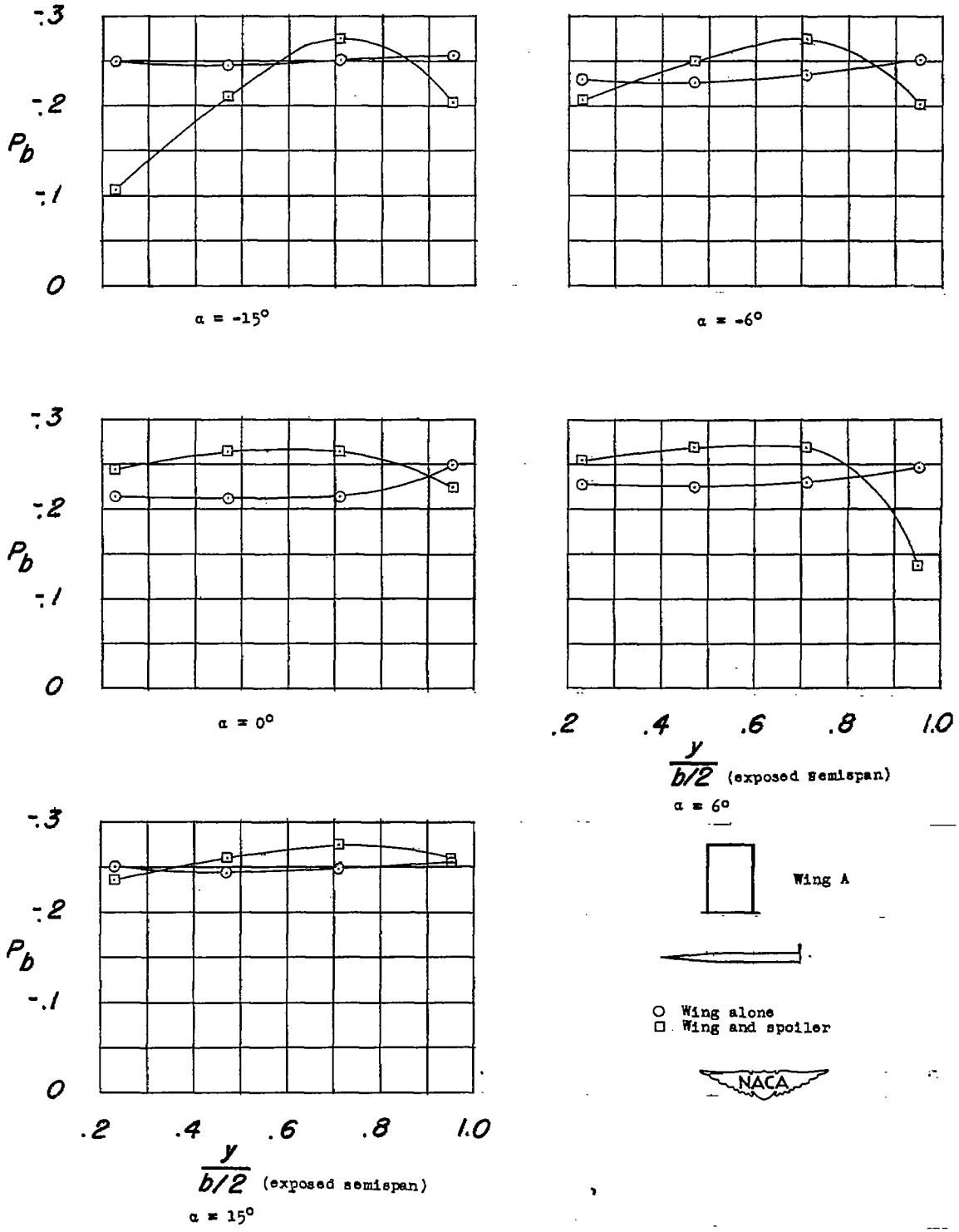

(b) M = 1.96; R = 1.3×10^6.

Figure 7.- Concluded.

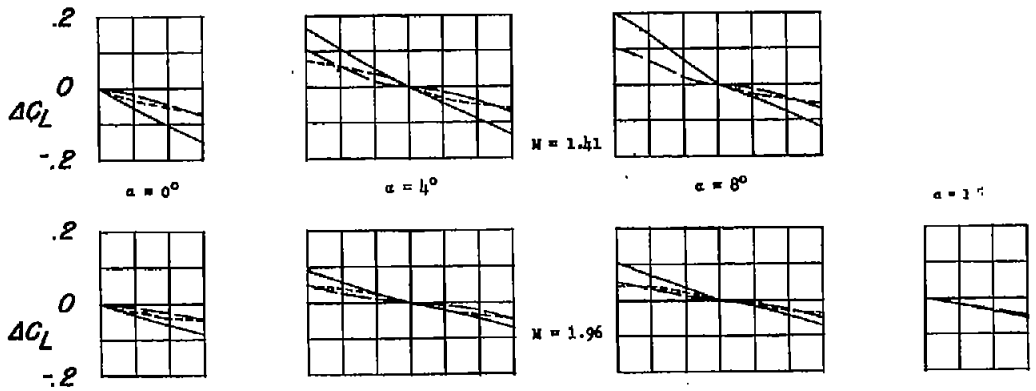

(a) Lift increment.

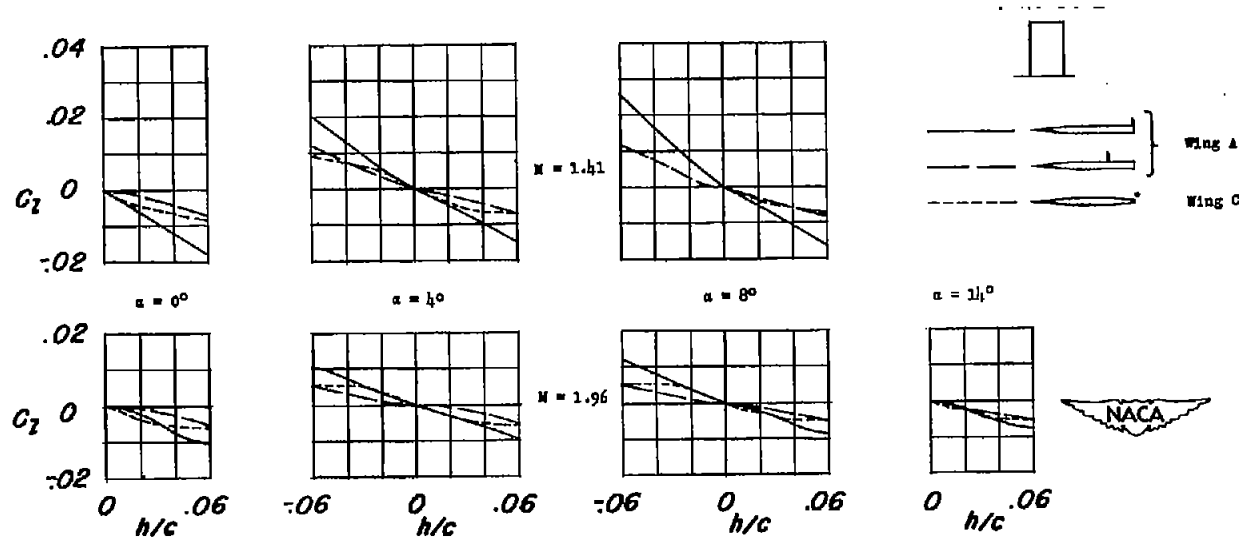

(b) Rolling moment.

Figure 8.- Increments in aerodynamic coefficients due to a spoiler projected at the 70-percent-chord line and at the trailing edge of an unswept semispan wing and increments due to pivoted spoiler located at the trailing edge of a related unswept semispan wing.

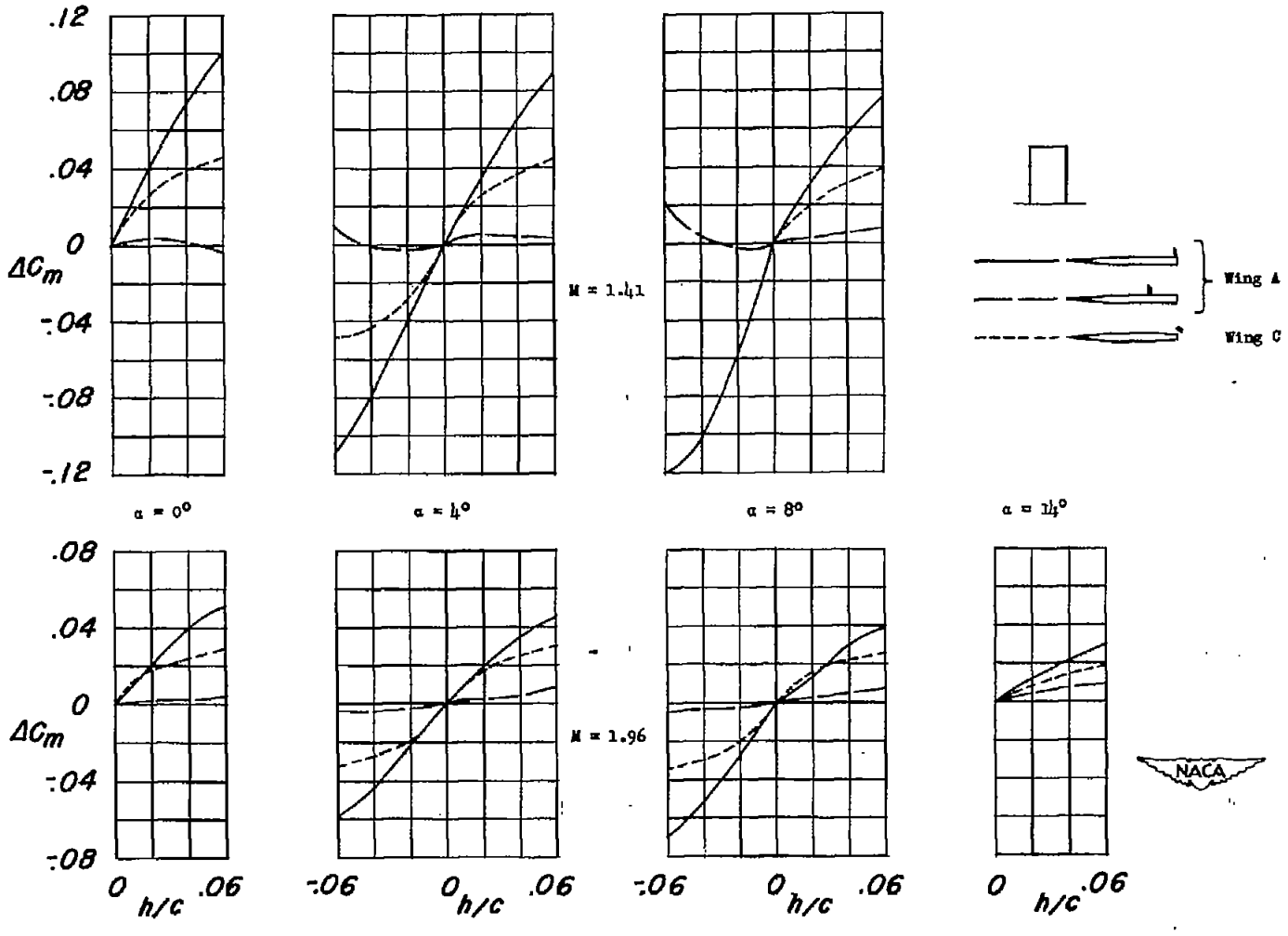

(c) Pitching-moment increment.

Figure 8.- Continued.

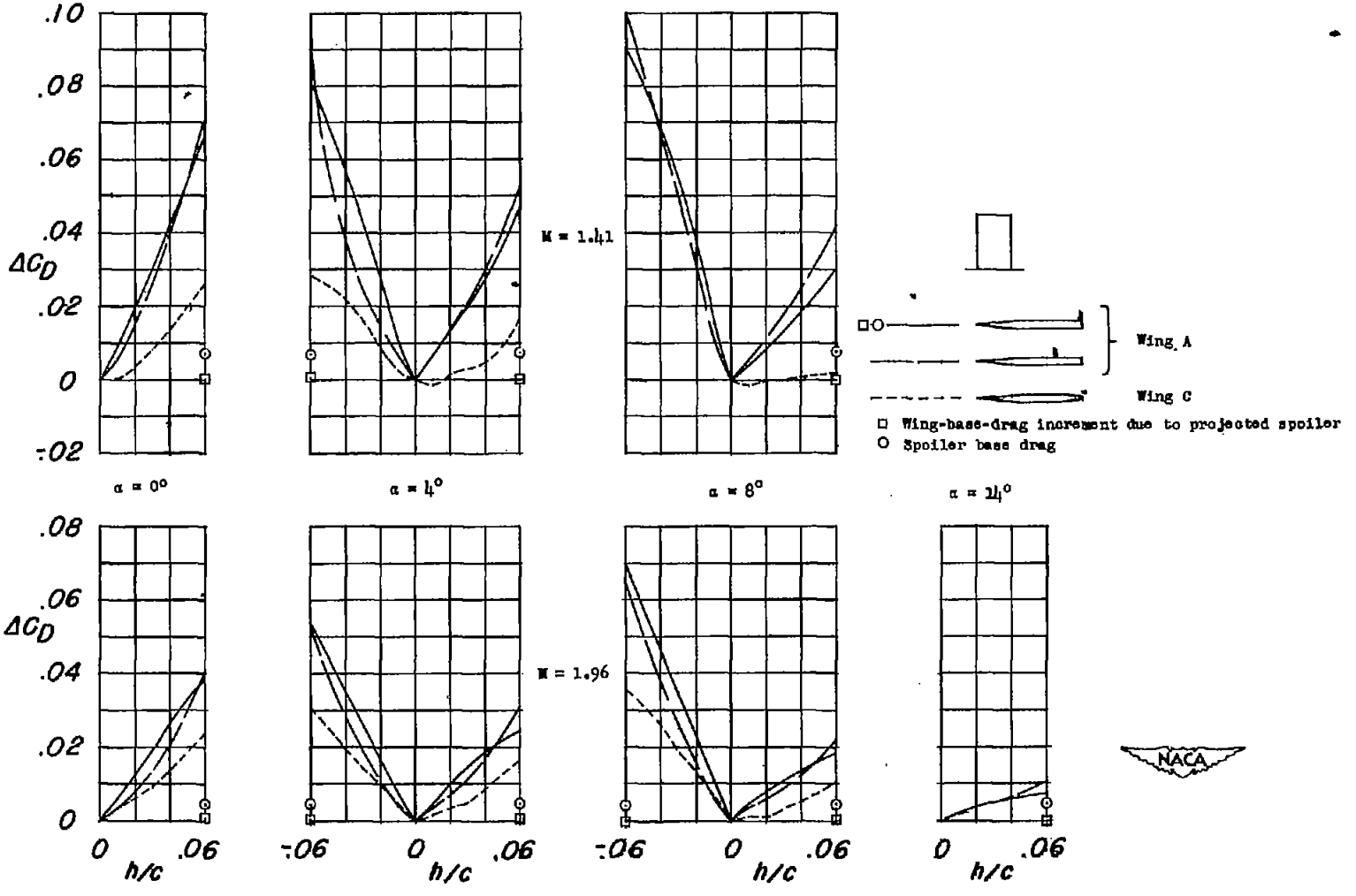

(d) Drag increment.

Figure 8.- Continued.

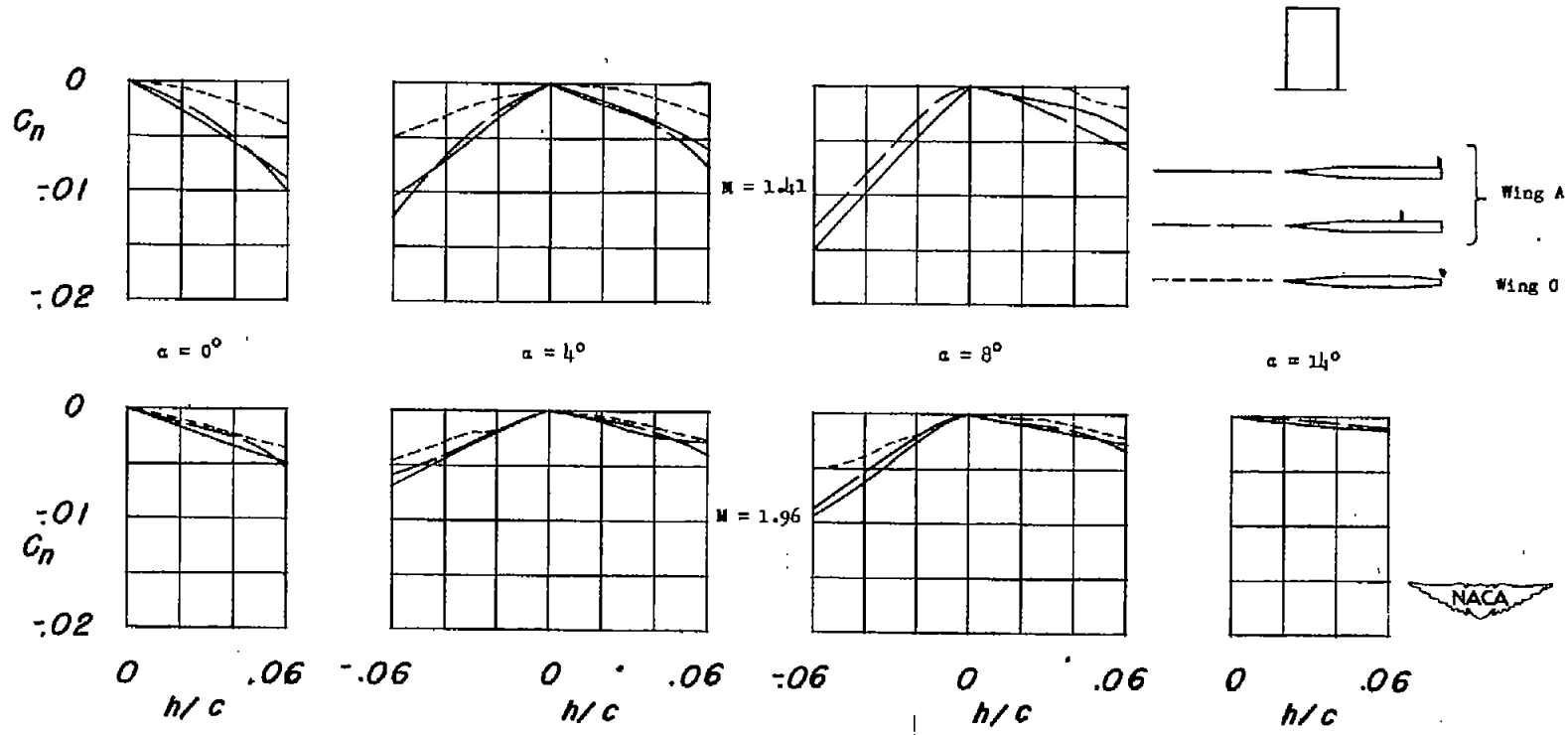

(e) Yawing moment.

Figure 8.- Concluded.

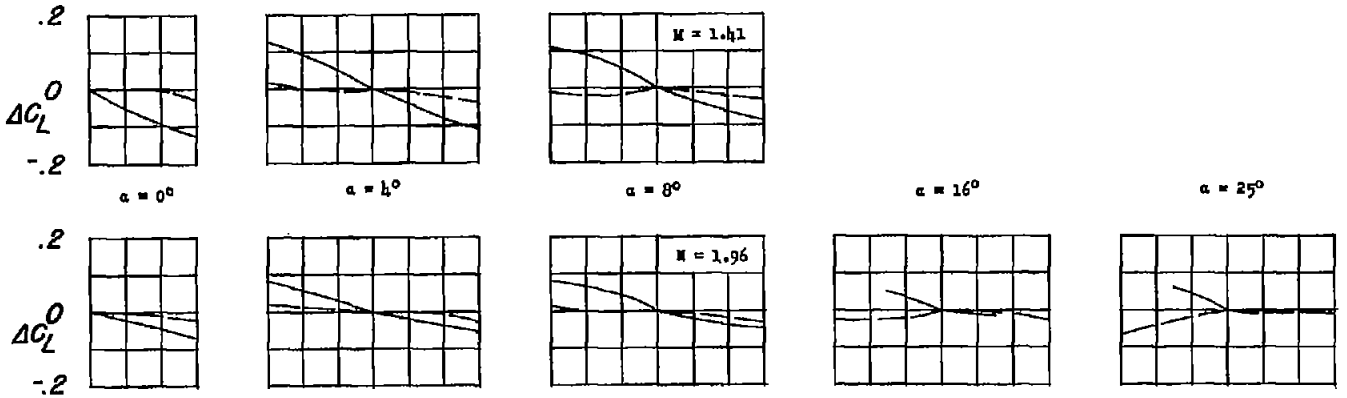

(a) Lift increment.

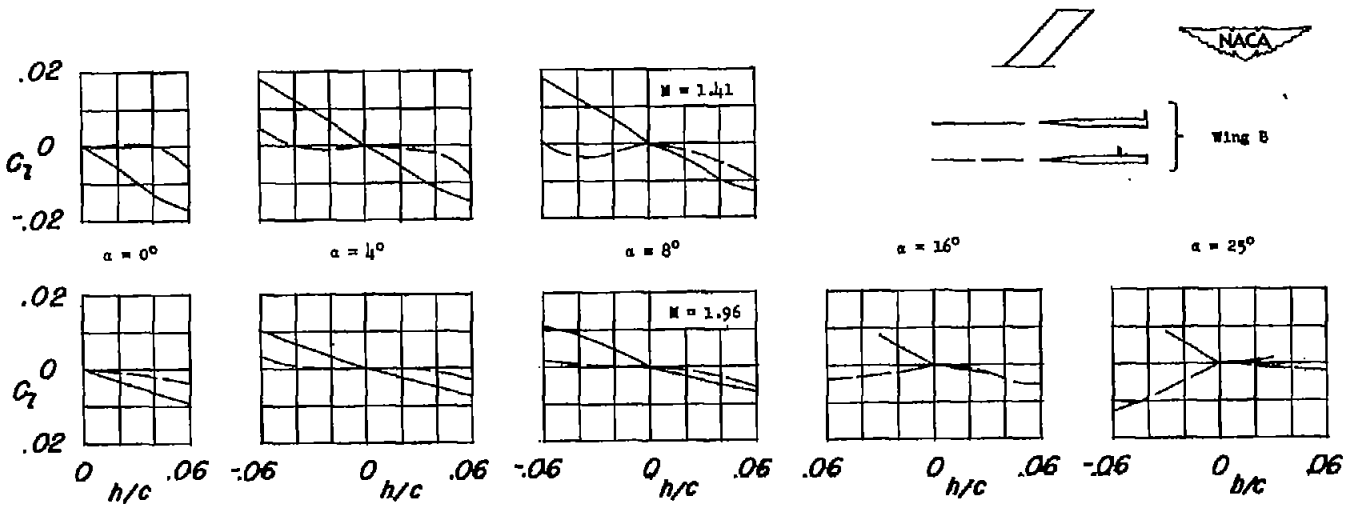

(b) Rolling moment.

Figure 9.- Increments in aerodynamic coefficients due to a spoiler projected at the 70-percent-chord line and at the trailing edge of a 45° sweptback semispan wing.

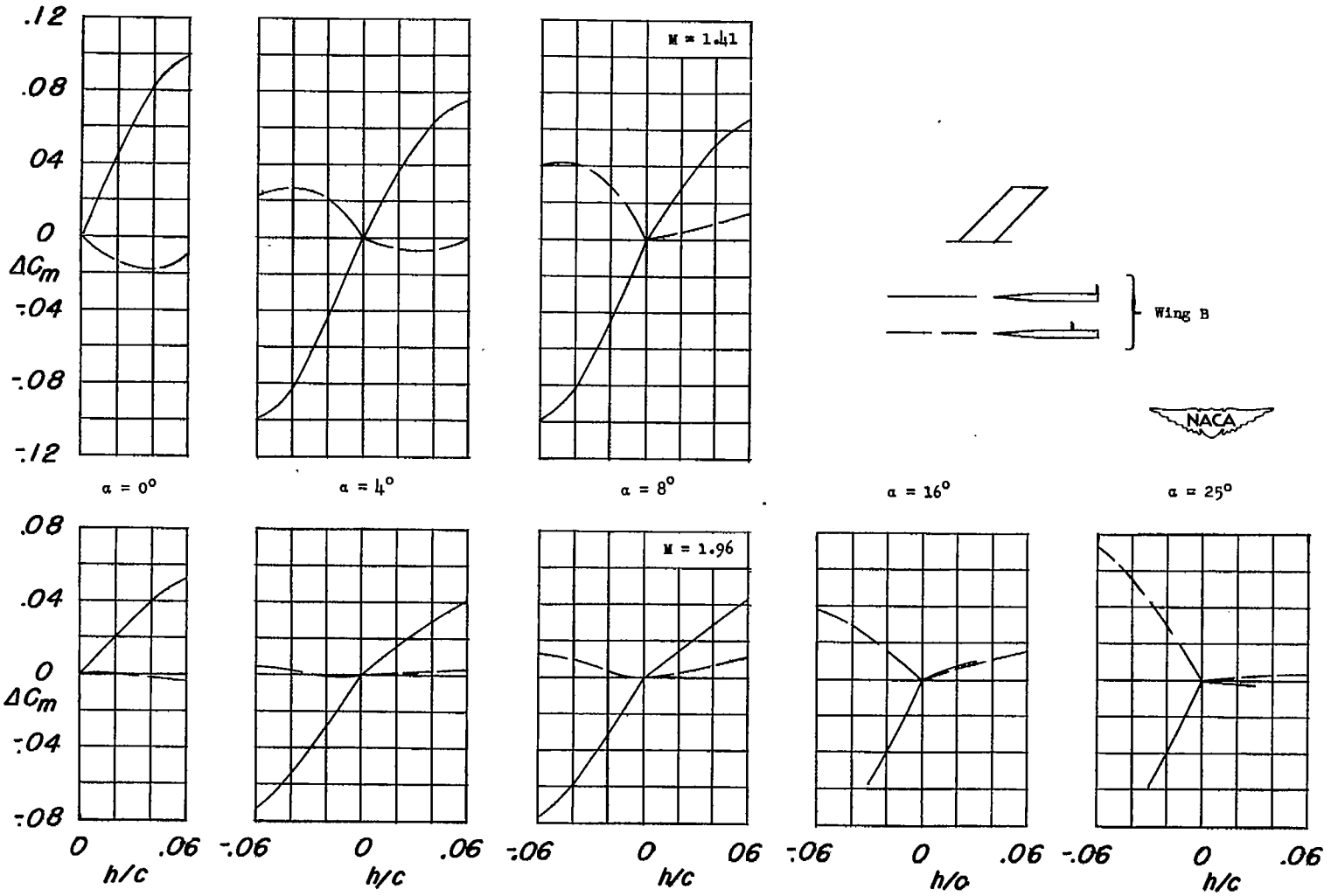

(c) Pitching-moment increment.

Figure 9.- Continued.

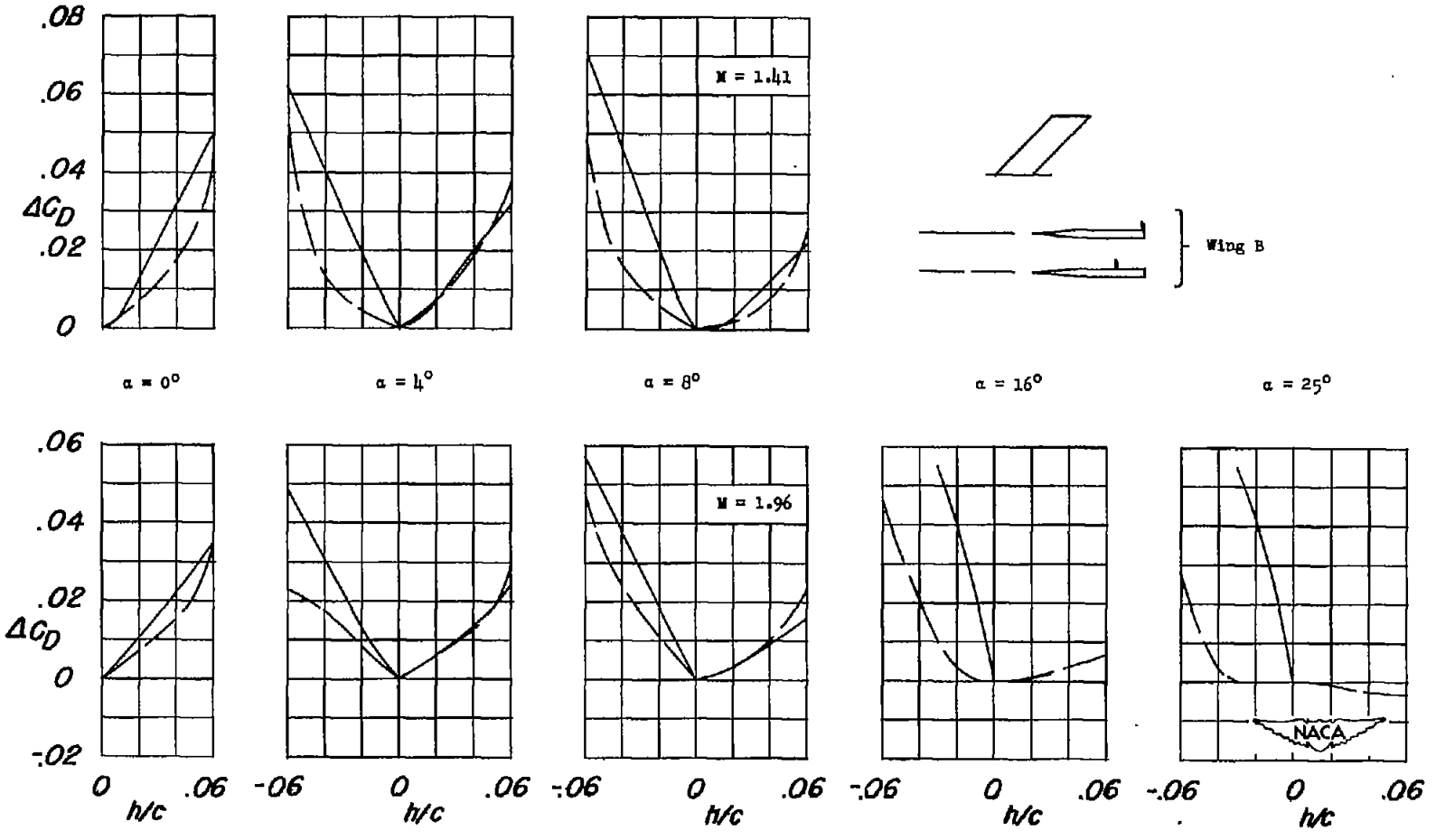

(d) Drag increment.

Figure 9.- Continued.

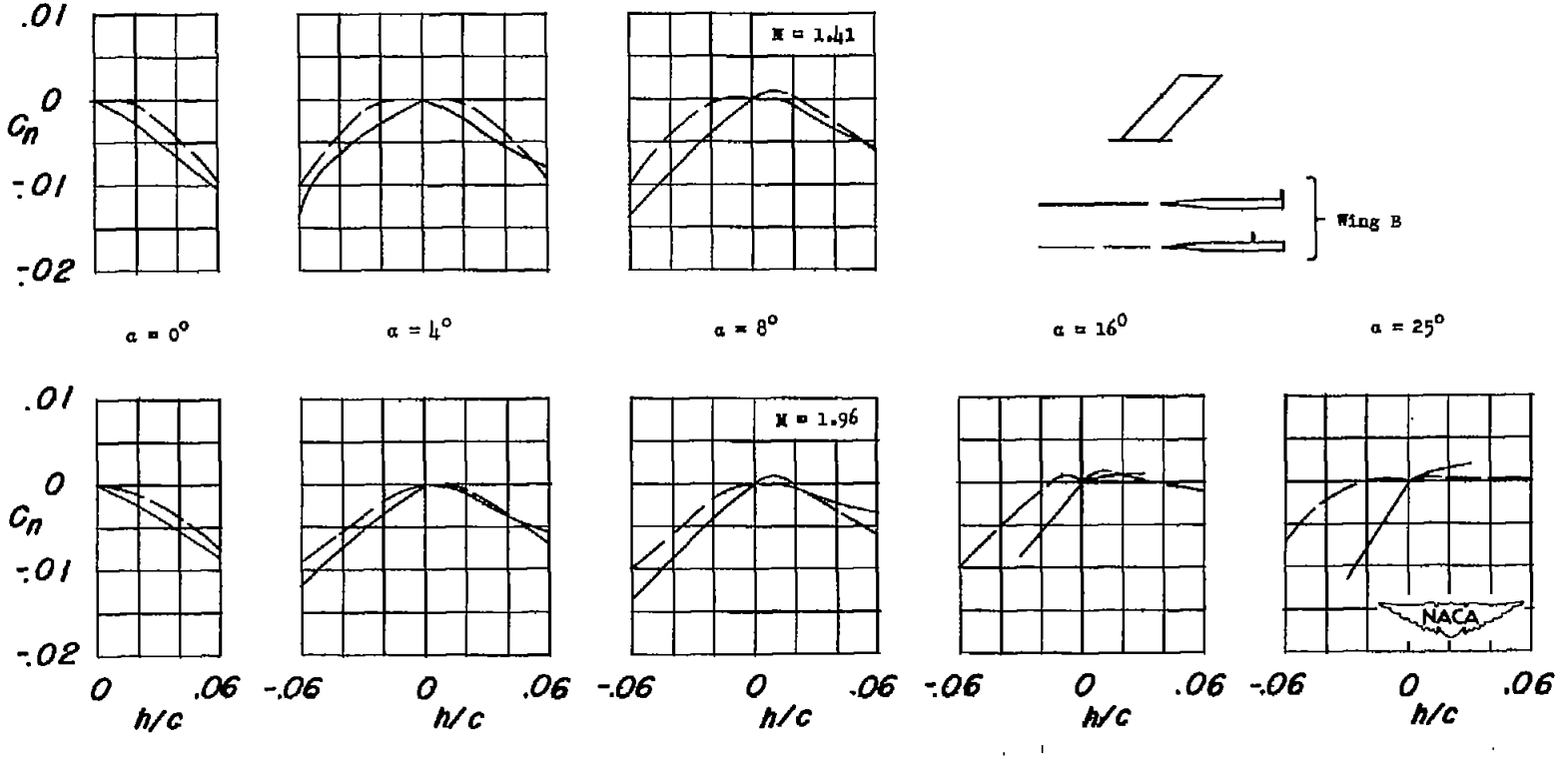

(e) Yawing moment.

Figure 9.- Concluded.

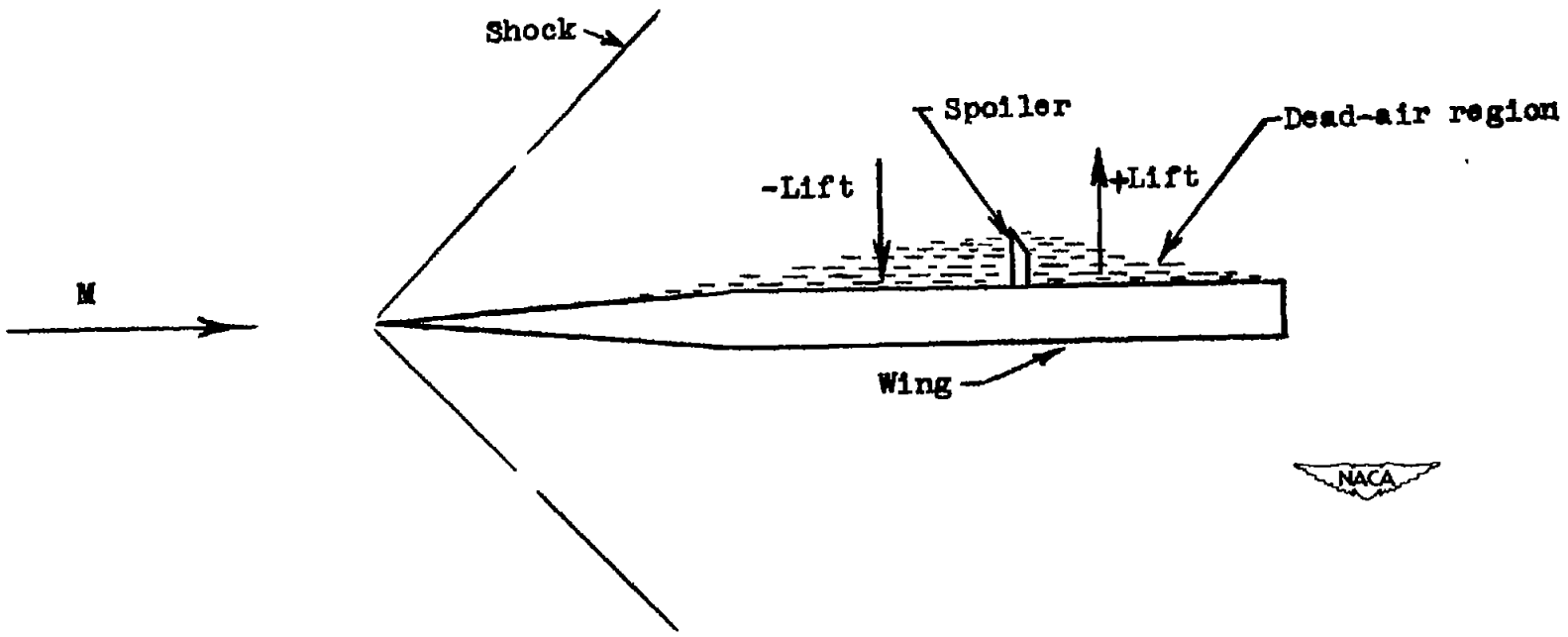

Figure 10.- Effect of a spoiler on the flow over a wing.